
Towards painless defibrillation:
virtual electrode theory of electrical
stimulation of the heart
Igor R. Efimov, Ph.D. F.A.H.A., F.H.R.S.
Cardiac Bioelectricity and Arrhythmia Center
Department of Biomedical Engineering
Washington University in St.Louis

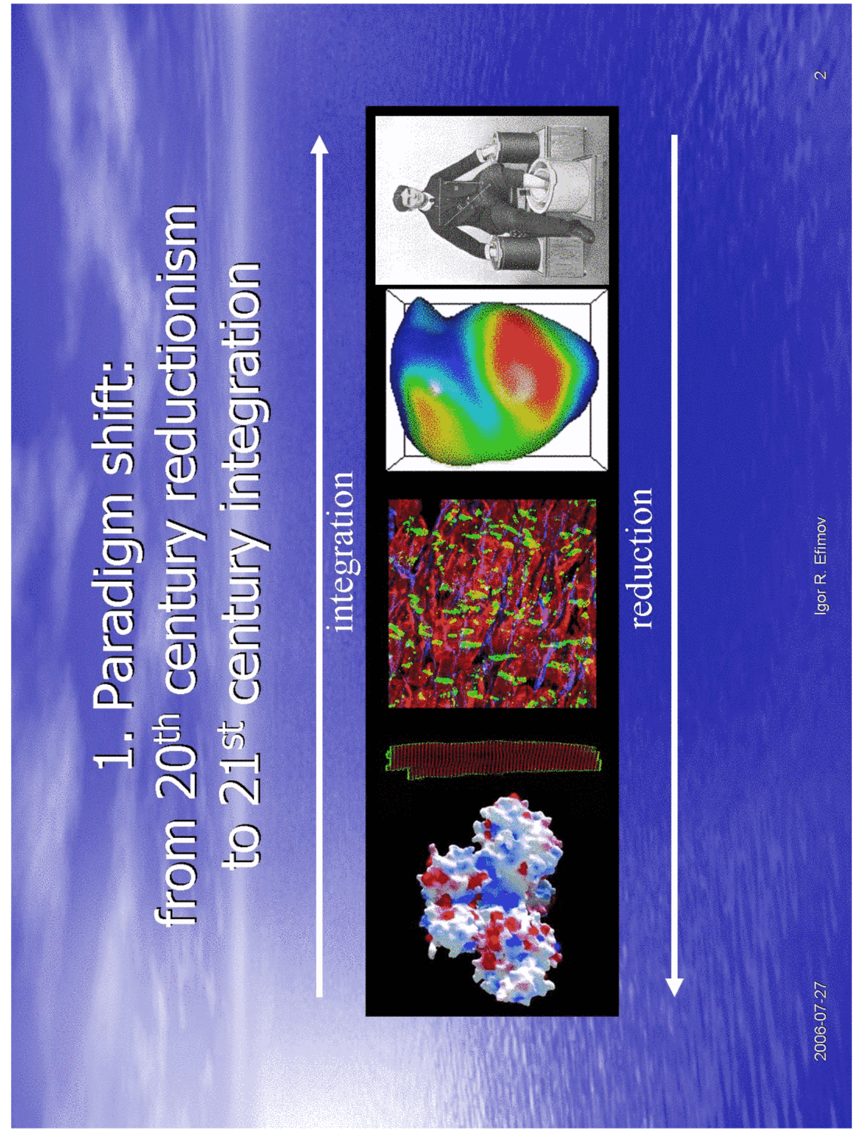
1. Paradigm shift:
from 20th century reductionism
to 21st century integration
integration
reduction
2006-07-27
Igor R. Efimov
2

Defibrillation: The Only Effective Therapy for Sudden Cardiac Death

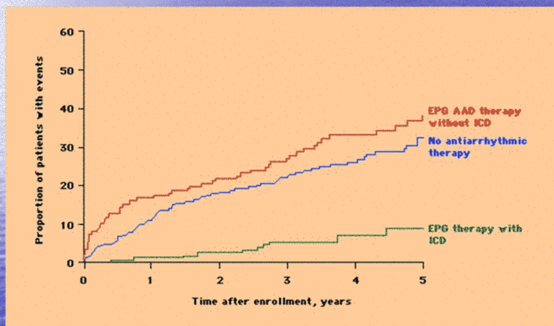

ICD reduces sudden death in MUSTT The MUSTT trial enrolled 704 patients with coronary artery disease, nonsustained ventricular tachycardia (VT) and a left ventricular ejection fraction ≤40 percent who had sustained VT induced during electrophysiologic (EP) study. Kaplan-Meier estimates show that the incidence of cardiac arrest or death from arrhythmia is significantly lower in those receiving an implantable cardioverter-defibrillator (ICD) compared to those receiving no therapy or those with EP-guided (EPG) antiarrhythmic drug (AAD) therapy. (Data from Buxton, AE, Lee, KL, Fisher, JD, et al, N Engl J Med 1999; 341:1882).

Annual Pacemaker and Implantable Cardioverter-Defibrillator (ICD) Implants in the United States

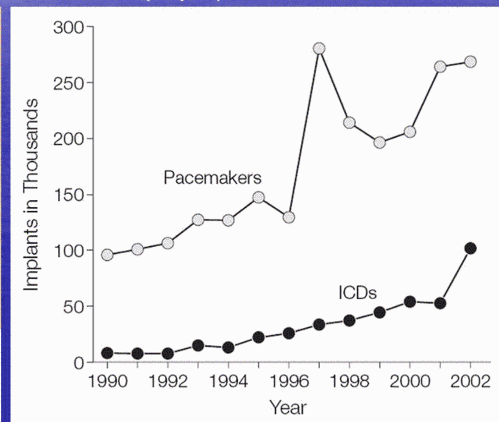

Maisel et al, Pacemaker and ICD Generator Malfunctions: Analysis of Food and Drug Administration Annual Reports, JAMA, 2006, 295: 1901-6.

Pacemaker and ICD Reliability and Complications

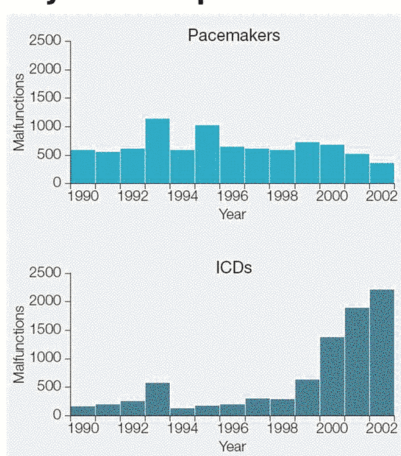

Reliability and complications of pacemakers and implantable cardioverter-defibrillators (ICDs) are the focus of 3 articles in this issue of *JAMA*. First, Maisel and colleagues reviewed manufacturers' reports of device malfunctions to the US Food and Drug Administration for 1990-2002 and found that pacemaker malfunctions declined during these years, but malfunctions of ICDs increased during the latter half of the study period. In the second article, Gould and Krahn surveyed Canadian centers that implant ICDs to assess complications associated with ICD generator replacement when manufacturers' advisories suggest a potential for device malfunction. These authors found that 8.1% of patients having ICD replacement experienced complications, including 2 deaths. In the third article, Maisel reports results of a meta-analysis of device registry data collected from 1983-2004 to assess annual rates of malfunction and trends. He found that pacemaker reliability improved over the period of analysis but reported a transient increase in the ICD malfunction rate from 1998-2002 followed by a substantial decrease through 2004. In an editorial, Wilkoff discusses the strengths and weaknesses of these data for informing patient and physician decisions regarding pacemaker or ICD replacement.

JAMA, 2006, 295.

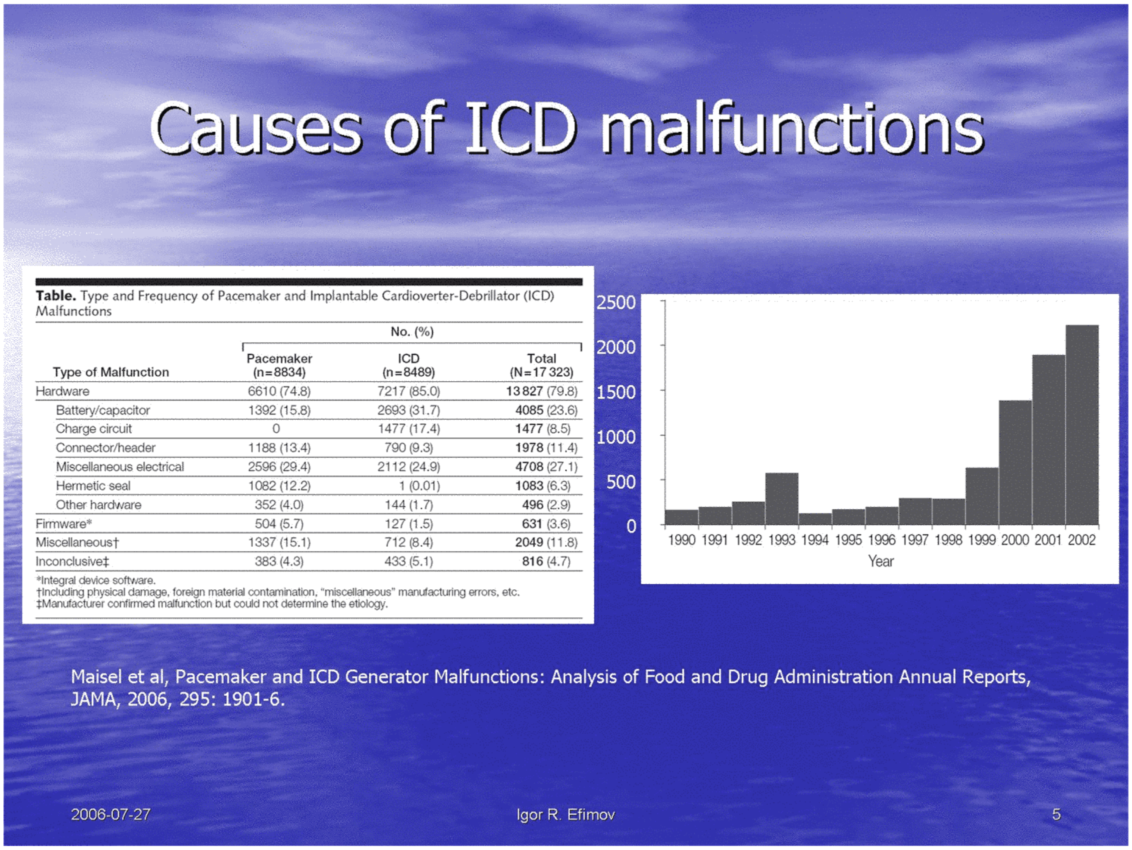

Table. Type and Frequency of Pacemaker and Implantable Cardioverter-Debrillator (ICD) Malfunctions

	No. (%)		
Type of Malfunction	Pacemaker (n=8834)	ICD (n=8489)	Total (N=17 323)
Hardware	6610 (74.8)	7217 (85.0)	13 827 (79.8)
Battery/capacitor	1392 (15.8)	2693 (31.7)	4085 (23.6)
Charge circuit	0	1477 (17.4)	1477 (8.5)
Connector/header	1188 (13.4)	790 (9.3)	1978 (11.4)
Miscellaneous electrical	2596 (29.4)	2112 (24.9)	4708 (27.1)
Hermetic seal	1082 (12.2)	1 (0.01)	1083 (6.3)
Other hardware	352 (4.0)	144 (1.7)	496 (2.9)
Firmware*	504 (5.7)	127 (1.5)	631 (3.6)
Miscellaneous†	1337 (15.1)	712 (8.4)	2049 (11.8)
Inconclusive‡	383 (4.3)	433 (5.1)	816 (4.7)

*Integral device software.
†Including physical damage, foreign material contamination, "miscellaneous" manufacturing errors, etc.
‡Manufacturer confirmed malfunction but could not determine the etiology.

Virtual electrode:

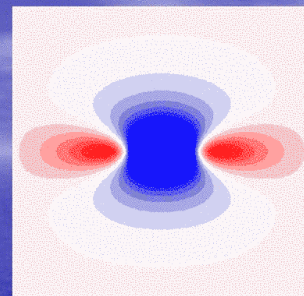

- Virtual electrode (S. Furman, 1967)
- Activating function (F. Rattay, 1987)
- Virtual electrodes during point stimulation (Sepulveda et al, 1989)
- Generalized activating function (Sobie et al, 1997)

Bidomain equations: Activating function

$$\nabla(\hat{g}_i \nabla \phi_i) = \beta(C_m \frac{\partial V_m}{\partial t} + I_{ion})$$

$$\phi_i = V_m + \phi_e$$

$$\nabla(\hat{g}_e \nabla \phi_e) = -\beta(C_m \frac{\partial V_m}{\partial t} + I_{ion})$$

Activating function

$$\beta(C_m \frac{\partial V_m}{\partial t} + I_{ion}) - \nabla \bullet (\hat{g}_i \nabla V_m) = \boxed{\nabla \bullet (\hat{g}_i \nabla \phi_e)}$$

Activating function at "rest"

(assume $I_{ion}=0$, $V_m=0$)

$$\beta(C_m \frac{\partial V_m}{\partial t} + I_{ion}) - \nabla \bullet (\hat{g}_i \nabla V_m) = \nabla \bullet (\hat{g}_i \nabla \phi_e) = S$$

$$S = \nabla \bullet (\hat{g}_i \nabla \phi_e) = \hat{g}_i \times \nabla(\nabla \phi_e) + (\nabla \bullet g_i) \bullet \nabla \phi_e$$

Field gradient $\sim g \frac{\partial^2 \phi_e}{\partial x^2}$

$\sim \frac{\partial g}{\partial x} \frac{\partial \phi_e}{\partial x}$ Myocardial heterogeneity

2006-07-27 Igor R. Efimov 9

Virtual electrode polarization in the near-field: bidomain model

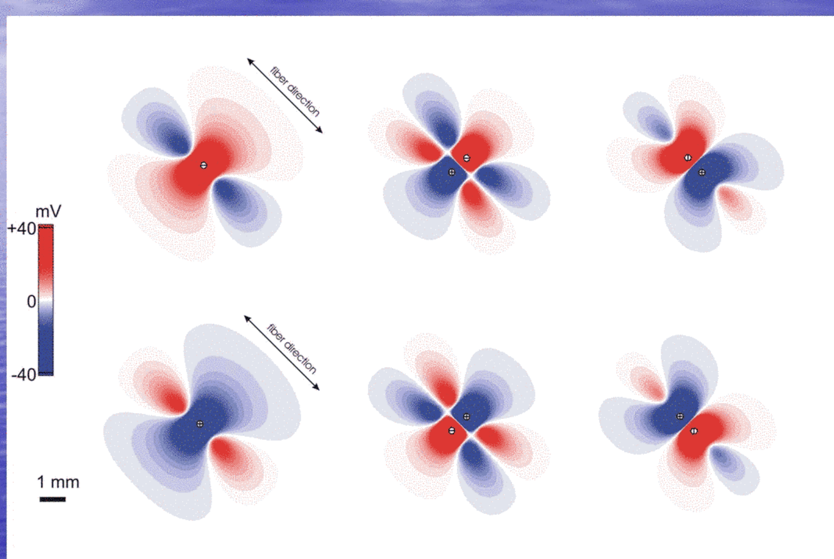

Nikolski et al, AJP, 2002

2006-07-27 Igor R. Efimov 10

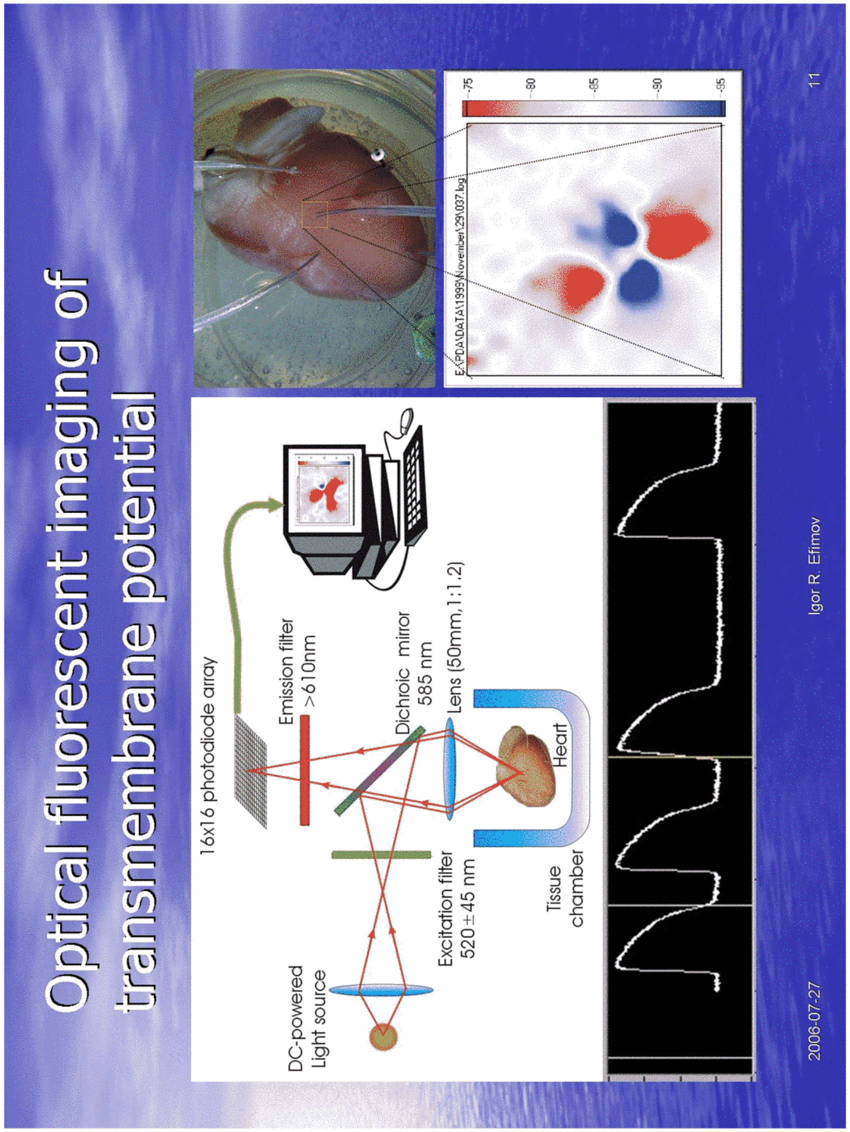
Optical fluorescent imaging of transmembrane potential
DC-powered Light source
Excitation filter 520 ± 45 nm
16x16 photodiode array
Emission filter >610nm
Dichroic mirror 585 nm
Lens (50mm,1:1.2)
Heart
Tissue chamber
2006-07-27
Igor R. Efimov
11

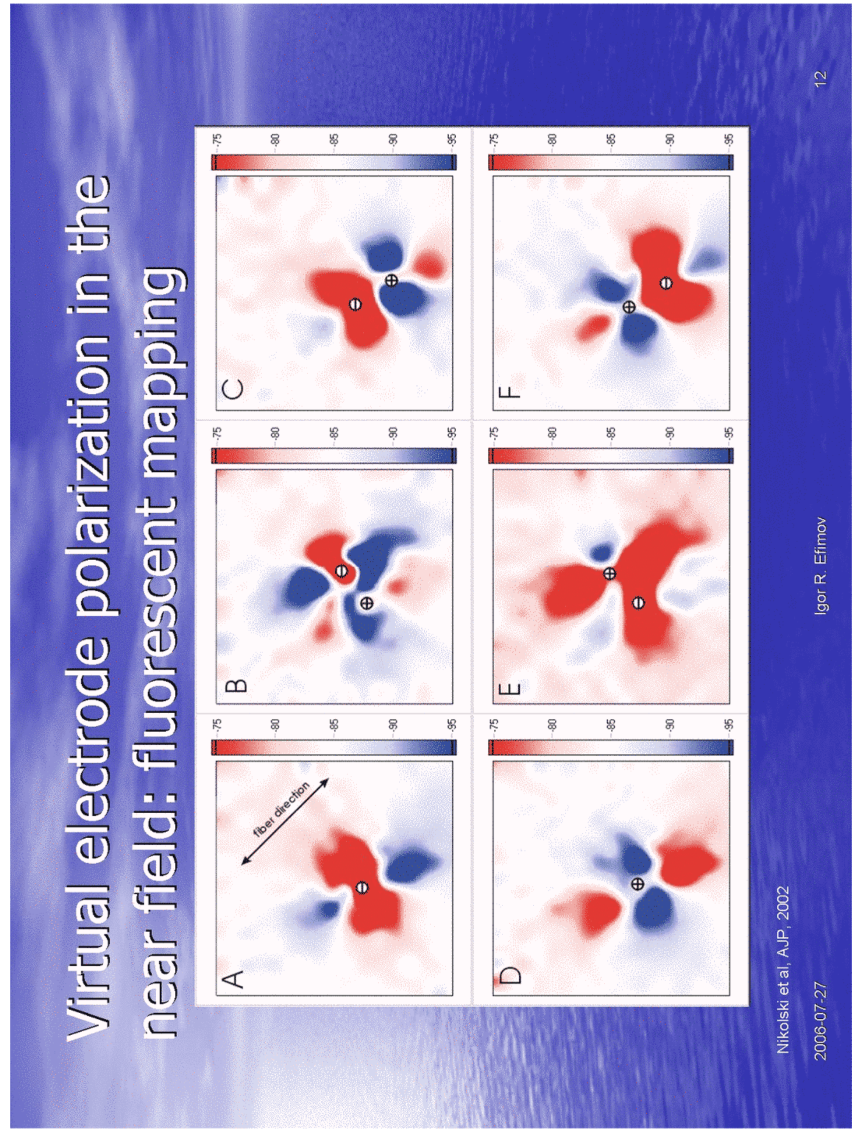
Virtual electrode polarization in the near field: fluorescent mapping
A
B
C
D
E
F
fiber direction
Nikolski et al, AJP, 2002
2006-07-27
Igor R. Efimov
12

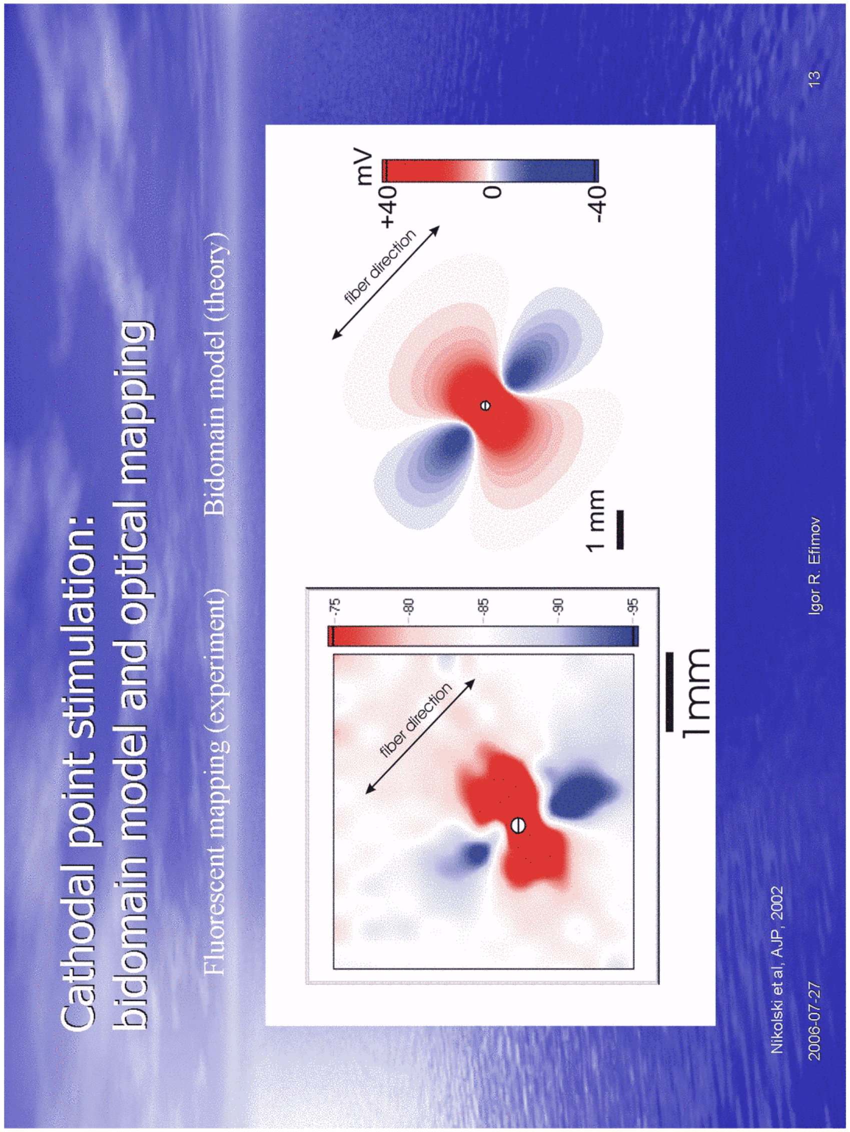
Cathodal point stimulation:
bidomain model and optical mapping
Fluorescent mapping (experiment)
Bidomain model (theory)
-75
-80
-85
-90
-95
fiber direction
1mm
fiber direction
+40
0
-40
mV
1 mm
Nikolski et al, AJP, 2002
2006-07-27
Igor R. Efimov
13

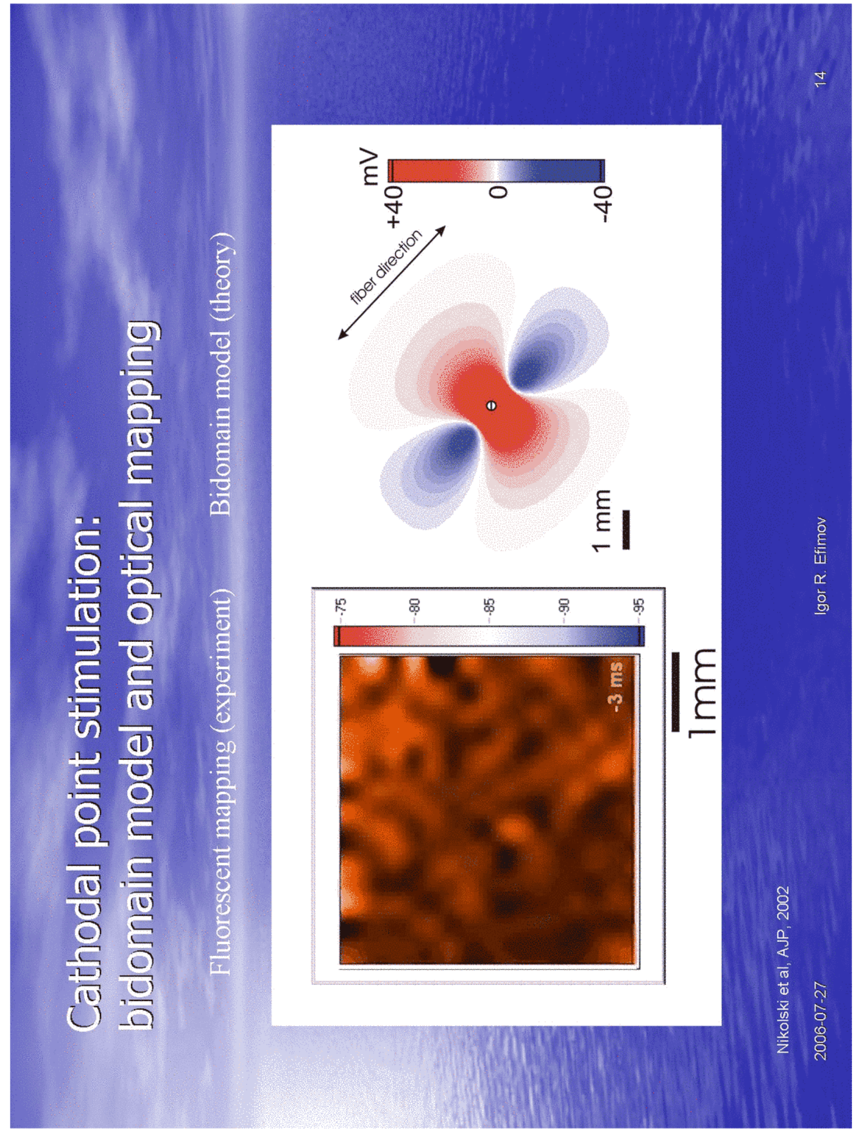
Cathodal point stimulation:
bidomain model and optical mapping
Fluorescent mapping (experiment)
Bidomain model (theory)
-75
-80
-85
-90
-95
-3 ms
1mm
fiber direction
+40
0
-40
mV
1 mm
Nikolski et al, AJP, 2002
2006-07-27
Igor R. Efimov
14


Virtual electrodes in the far-field
anode
cathode
V_m (mV)
-75 -45 -15 15 45 75
Efimov et al, AJP, 2000
2006-07-27
Igor R. Efimov
15

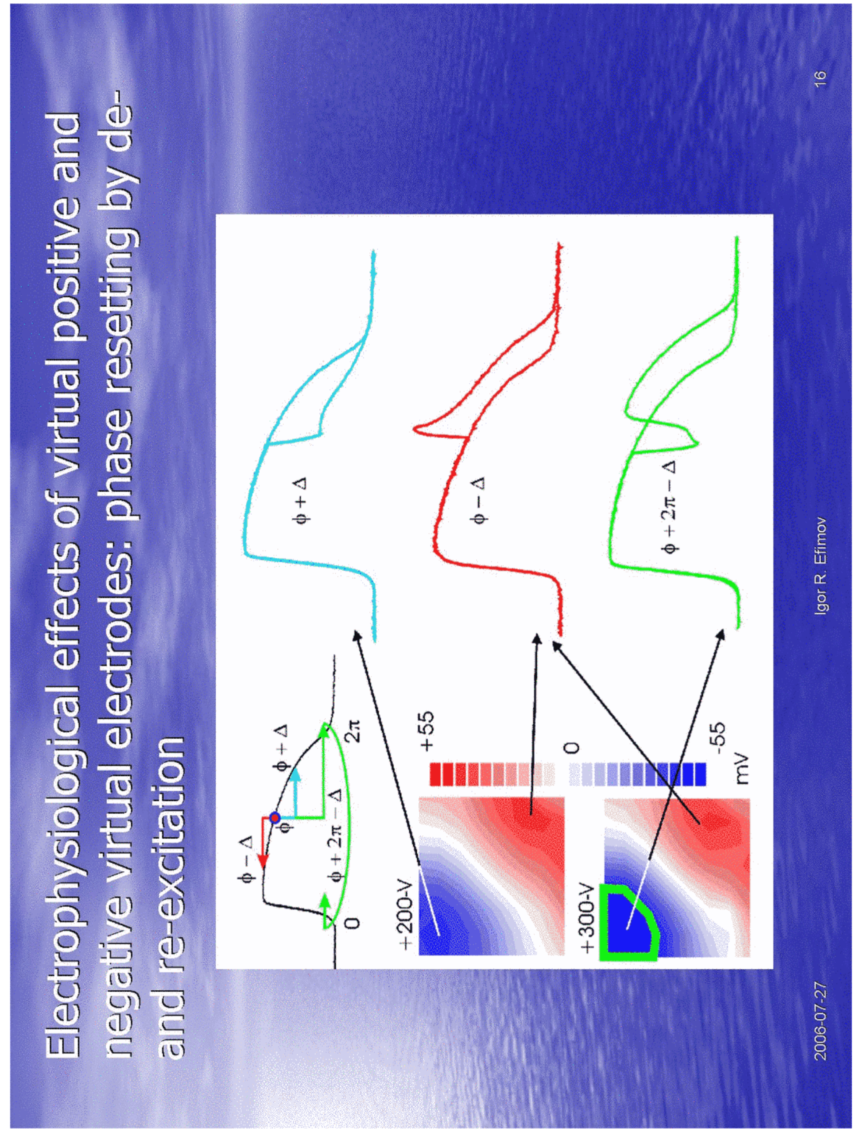
Electrophysiological effects of virtual positive and negative virtual electrodes: phase resetting by de- and re-excitation
φ − Δ
φ
φ + Δ
φ + 2π − Δ
0
2π
+200-V
+300-V
+55
0
-55
mV
φ + Δ
φ − Δ
φ + 2π − Δ
2006-07-27
Igor R. Efimov
16

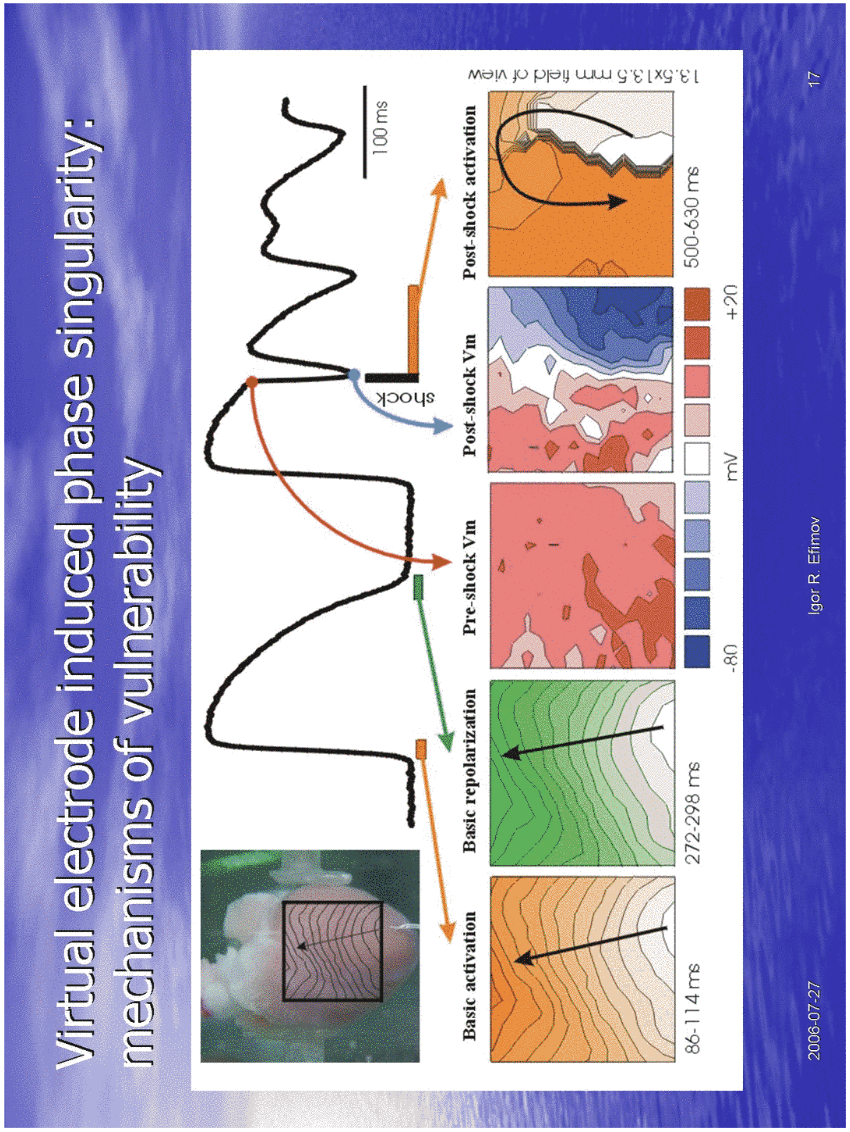
Virtual electrode induced phase singularity:
mechanisms of vulnerability
100 ms
shock
Basic activation
Basic repolarization
Pre-shock Vm
Post-shock Vm
Post-shock activation
86-114 ms
272-298 ms
-80
mV
+20
500-630 ms
13.5x13.5 mm field of view
2006-07-27
Igor R. Efimov
17

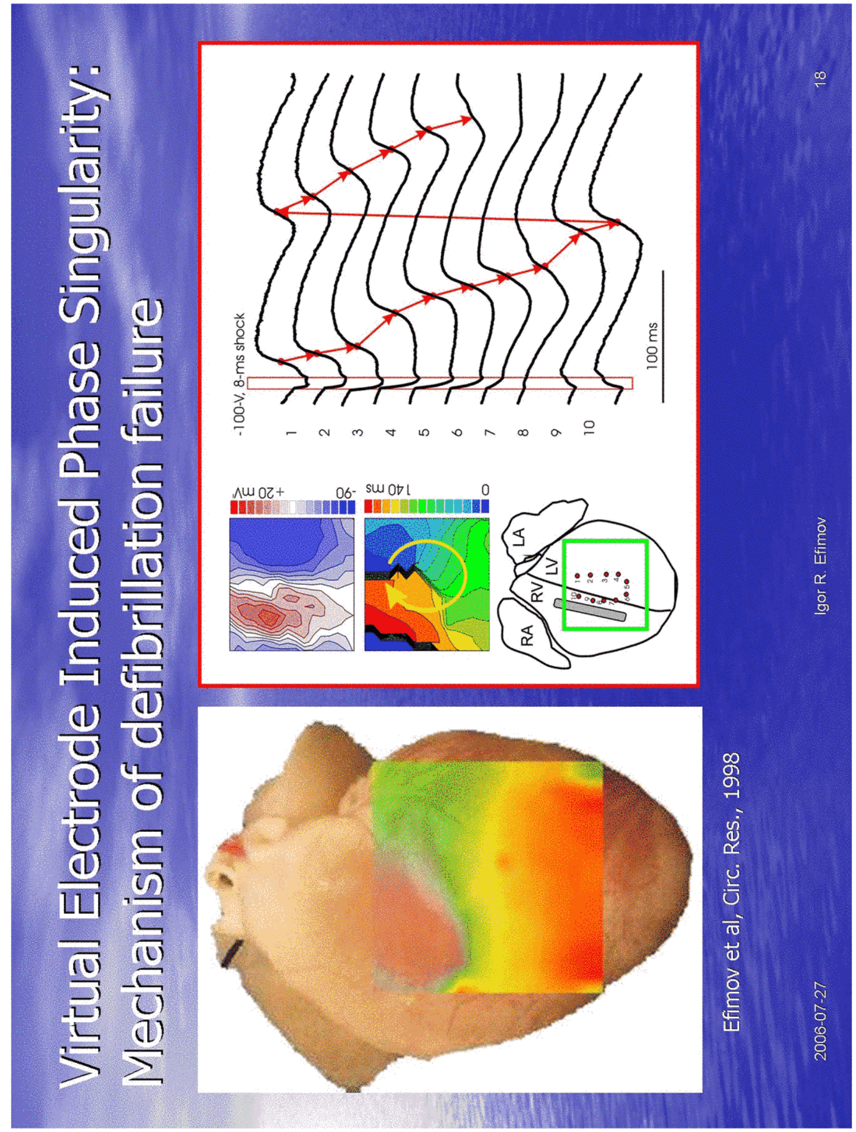
Virtual Electrode Induced Phase Singularity:
Mechanism of defibrillation failure
Efimov et al, Circ. Res., 1998
+20 mV
-90
140 ms
0
LA
LV
RV
RA
-100-V, 8-ms shock
1
2
3
4
5
6
7
8
9
10
100 ms
2006-07-27
Igor R. Efimov
18


Mechanisms of defibrillation:
1. Shock must terminate wavefronts that sustain VT/VF
2. Shock must not induce new wavefronts, which may result in new VT/VF
3. Shock must suppress sources of VT/VF (?)
4. Shock must not suppress post-shock recovery of the normal sinus rhythm
2006-07-27
Igor R. Efimov
19


3. Clinical implication of the Virtual Electrode Theory of Defibrillation
2006-07-27
Igor R. Efimov
20

Virtual Electrode Theory of Defibrillation explained:

- The lower and upper limits of vulnerability
- Superiority of anodal versus cathodal shocks
- Superiority of biphasic over monophasic shocks
- Superiority of ascending versus descending waveforms

Conduction velocity of the wavefront determines completion of the first reentrant circuit

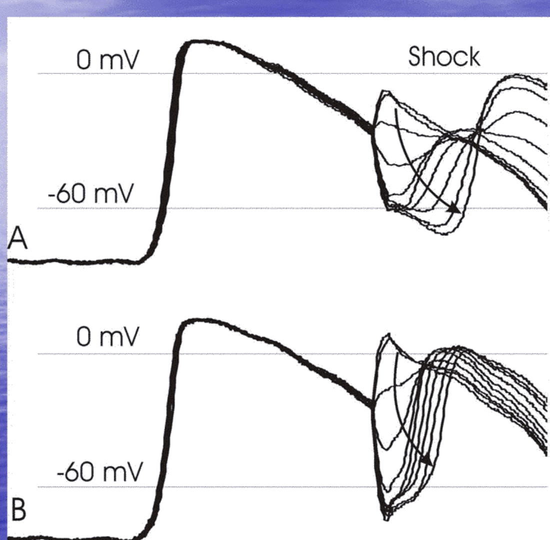

Optical recordings below the upper limit of vulnerability

and above the upper limit of vulnerability

Cheng et al, 2000

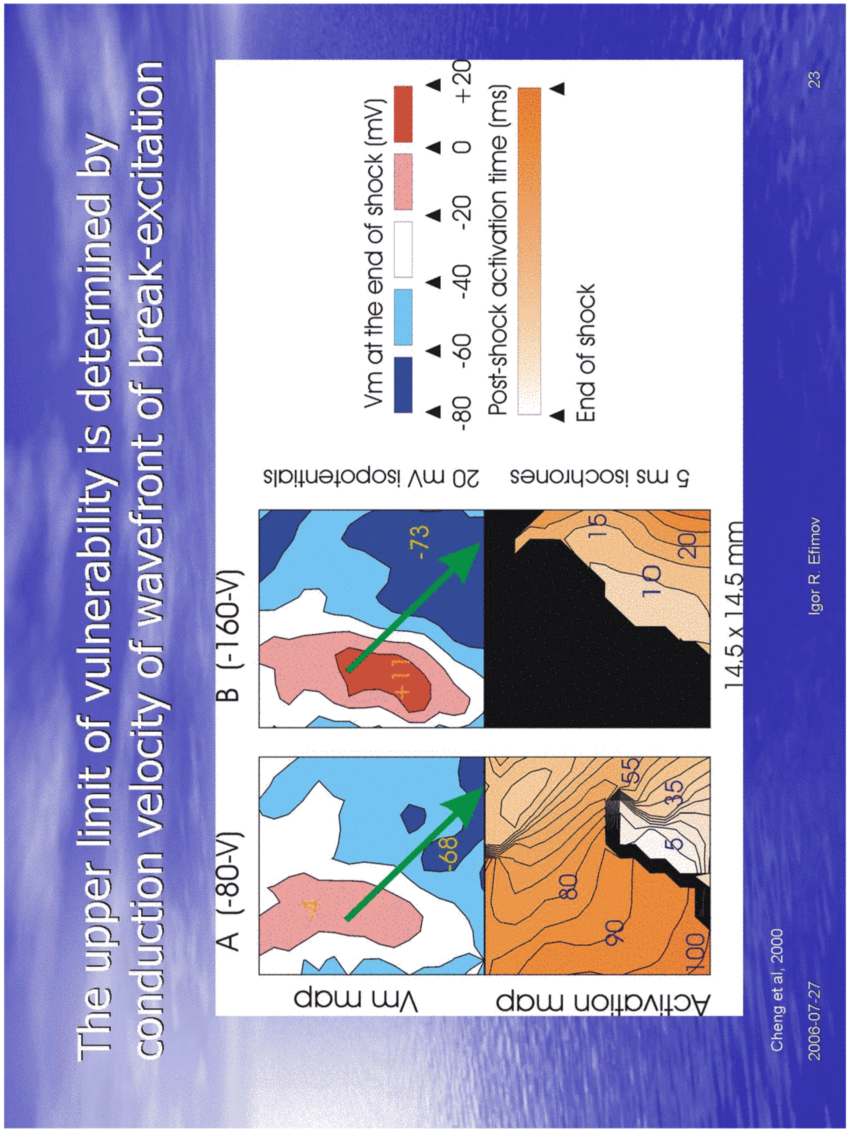
The upper limit of vulnerability is determined by conduction velocity of wavefront of break-excitation
A (-80-V)
B (-160-V)
Vm map
Activation map
20 mV isopotentials
5 ms isochrones
14.5 x 14.5 mm
Vm at the end of shock (mV)
-80 -60 -40 -20 0 +20
Post-shock activation time (ms)
End of shock
Cheng et al, 2000
2006-07-27
Igor R. Efimov
23

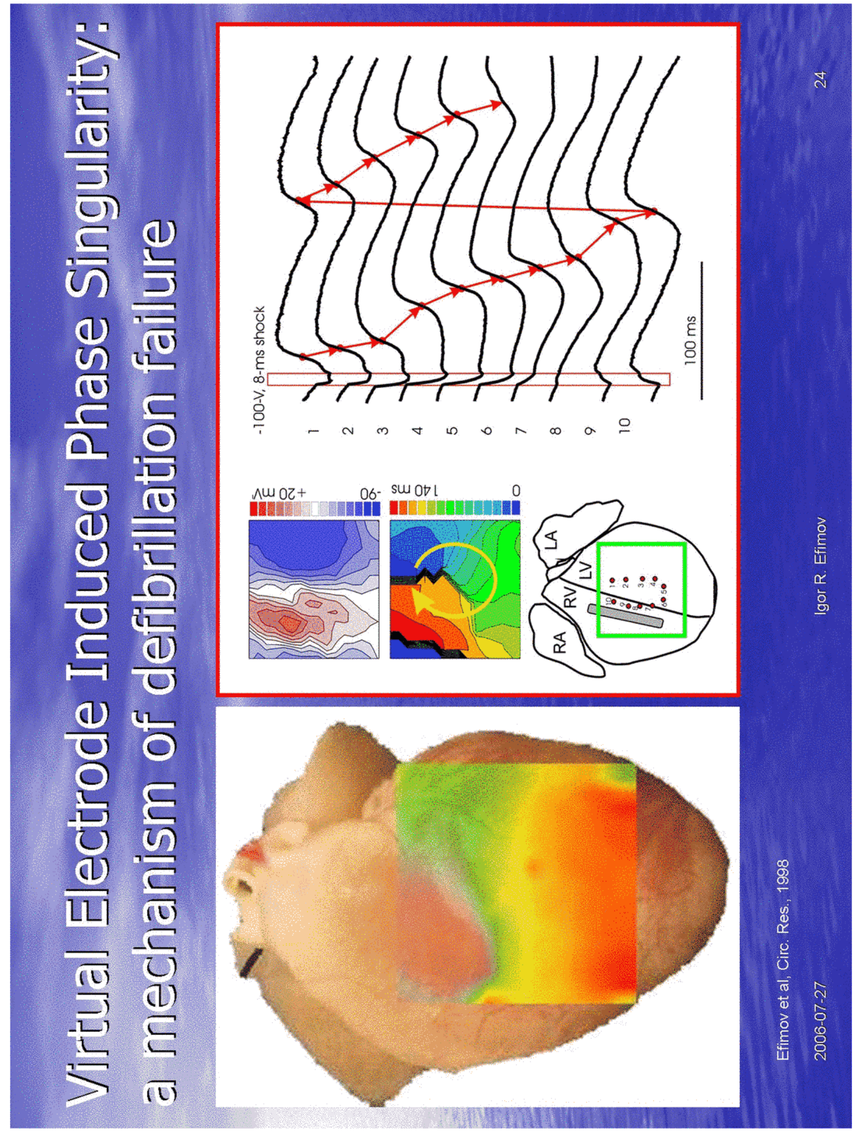
Virtual Electrode Induced Phase Singularity: a mechanism of defibrillation failure
-100-V, 8-ms shock
1 2 3 4 5 6 7 8 9 10
100 ms
+20 mV
-90
140 ms
0
RA
RV
LV
LA
Efimov et al, Circ. Res., 1998
2006-07-27
Igor R. Efimov
24

History of waveform optimization

- 1899: J.-L. Prevost and F. Battelli demonstrated both AC and DC (capacitor discharge) defibrillation
- 1930-1940s: C.J. Wiggers and C.S. Beck used 0.5-1.0 second AC shocks to achieve first successful clinical defibrillation
- 1939: N.L. Gurvich showed that DC (capacitor discharge + inductor) waveform is superior to AC
- 1960s: N.L. Gurvich presented optimized biphasic waveform, which was implemented in 1970 as a standard waveform for external defibrillators
- 1990s: Biphasic capacitor discharge waveform is staandard in all types of defibrillators: external, internal, and AED

Optimization of defibrillation waveform (20-60% improvement at a time)

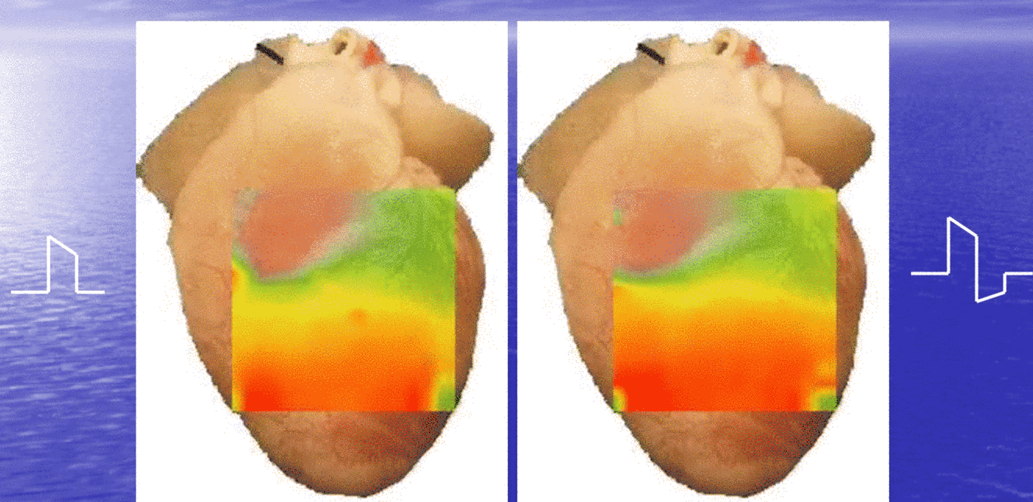

Monophasic shock Biphasic shock

Efimov et al, 1998-2000

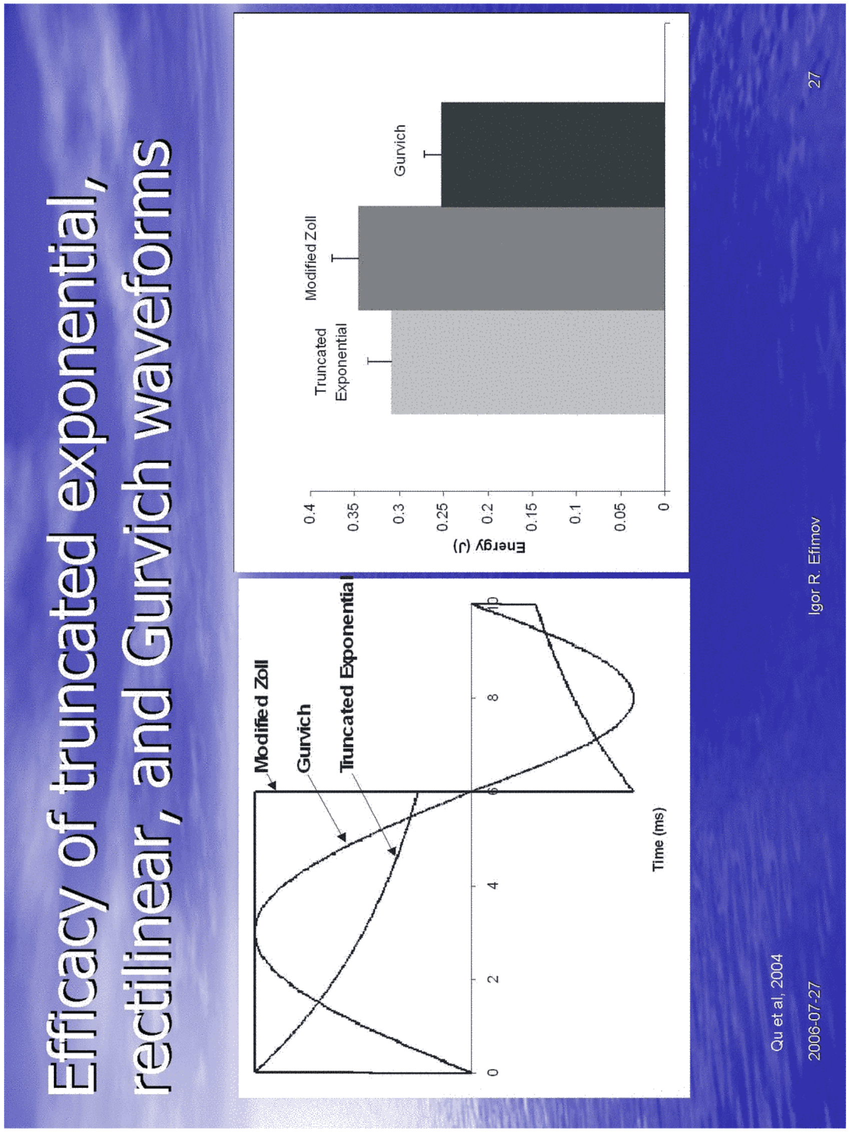
Efficacy of truncated exponential, rectilinear, and Gurvich waveforms
Modified Zoll
Gurvich
Truncated Exponential
Time (ms)
Energy (J)
Truncated Exponential
Modified Zoll
Gurvich
Qu et al, 2004
2006-07-27
Igor R. Efimov
27

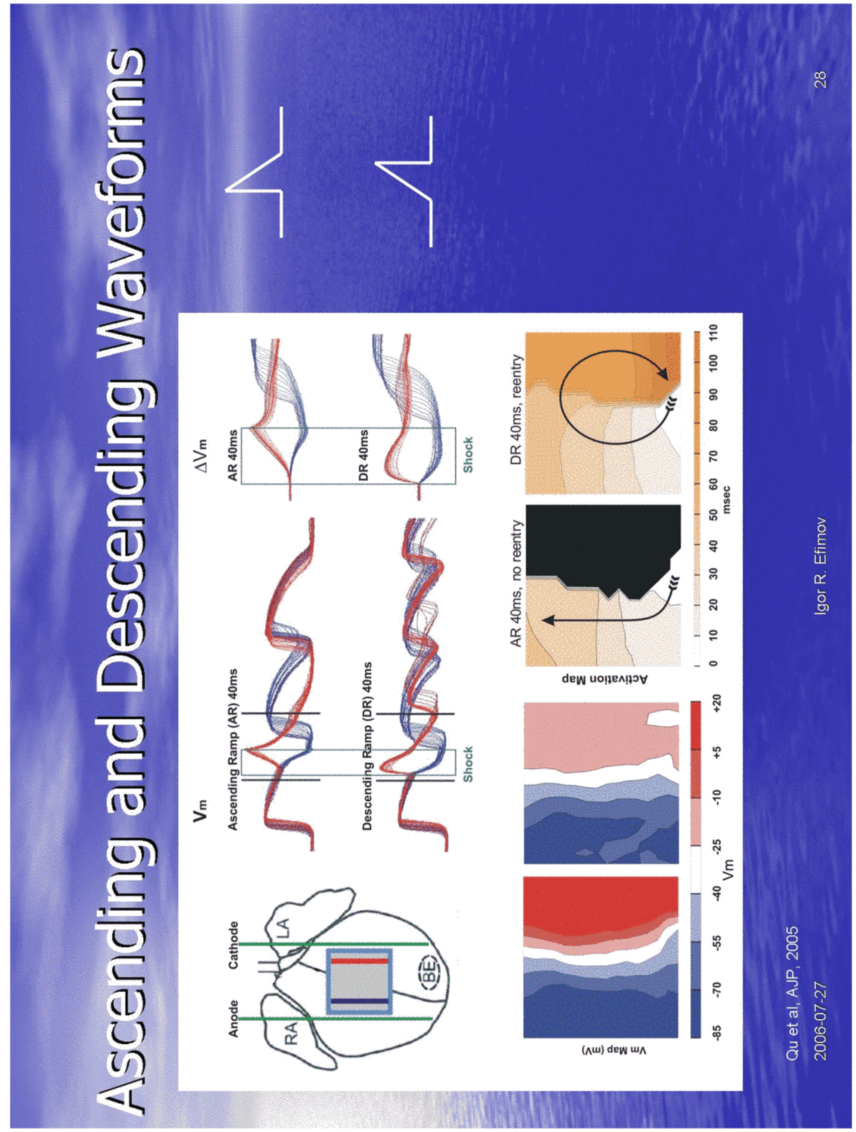
Ascending and Descending Waveforms
Anode
Cathode
LA
RA
BE
Vm
Ascending Ramp (AR) 40ms
Descending Ramp (DR) 40ms
Shock
ΔVm
AR 40ms
DR 40ms
Shock
Vm Map (mV)
Activation Map
AR 40ms, no reentry
DR 40ms, reentry
msec
Qu et al, AJP, 2005
2006-07-27
Igor R. Efimov
28

Clinical Superiority of Ascending Ramp Waveform

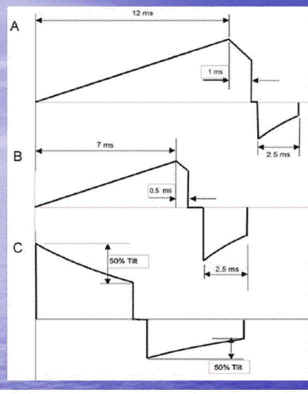

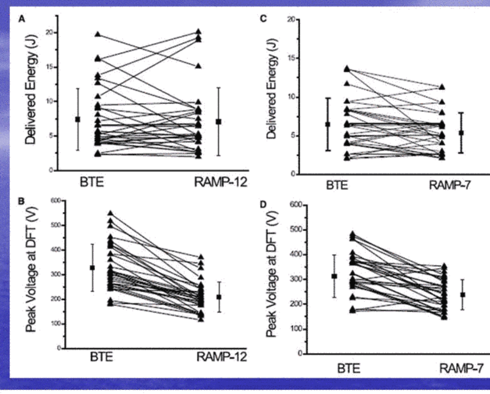

Table 2 Summary data at defibrillation threshold for each group of patients

	Biphasic truncated exponential waveform	Ramp waveform	Difference (%)	*P* value
Group 1 (12-ms ramp; n = 32)				
Delivered energy (J)	7.4 ± 4.5	7.1 ± 4.9	−2%	NS
Peak voltage (V)	327 ± 96	209 ± 61	−34%	<.001
Resistance (Ω)	36.2 ± 4.7	37.2 ± 5.2	2.7%	<.001
ULV delivered energy (J)	7.9 ± 4.6	7.7 ± 4.2	−0.4%	NS
Group 2 (7-ms ramp; n = 31)				
Total delivered energy (J)	6.5 ± 3.4	5.4 ± 2.6	−18%	<.02
Peak voltage (V)	313 ± 85	239 ± 62	−24%	<.01
Resistance (Ω)	39.1 ± 7.2	39.3 ± 7.1	−0.2%	NS
ULV delivered energy (J)	7.6 ± 3.7	7.0 ± 3.6	−8%	<.01

ULV, upper limit of vulnerability.

Shorofsky et al. Heart Rhythm 2005

2006-07-27 Igor R. Efimov 29

4. Side-effects of defibrillation: Further improvement is needed.

2006-07-27 Igor R. Efimov 30

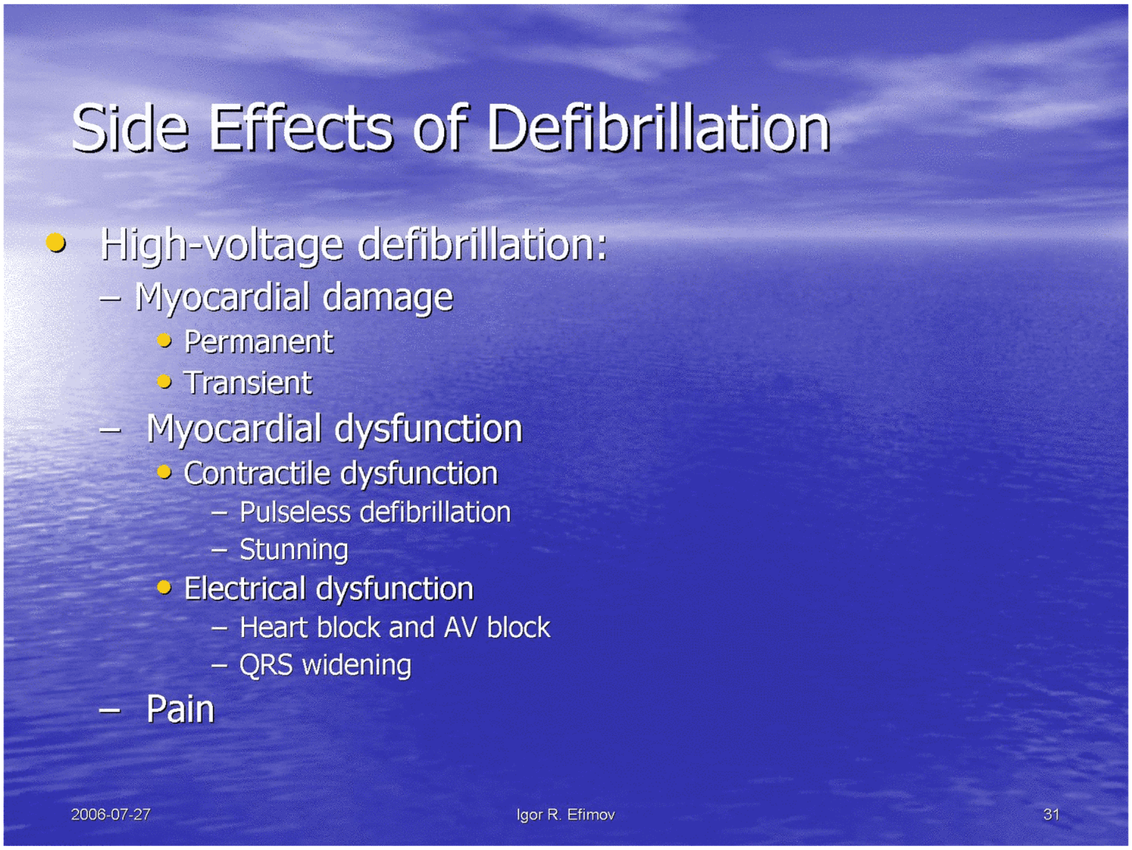
Side Effects of Defibrillation
High-voltage defibrillation:
– Myocardial damage
Permanent
Transient
– Myocardial dysfunction
Contractile dysfunction
– Pulseless defibrillation
– Stunning
Electrical dysfunction
– Heart block and AV block
– QRS widening
– Pain
2006-07-27
Igor R. Efimov
31

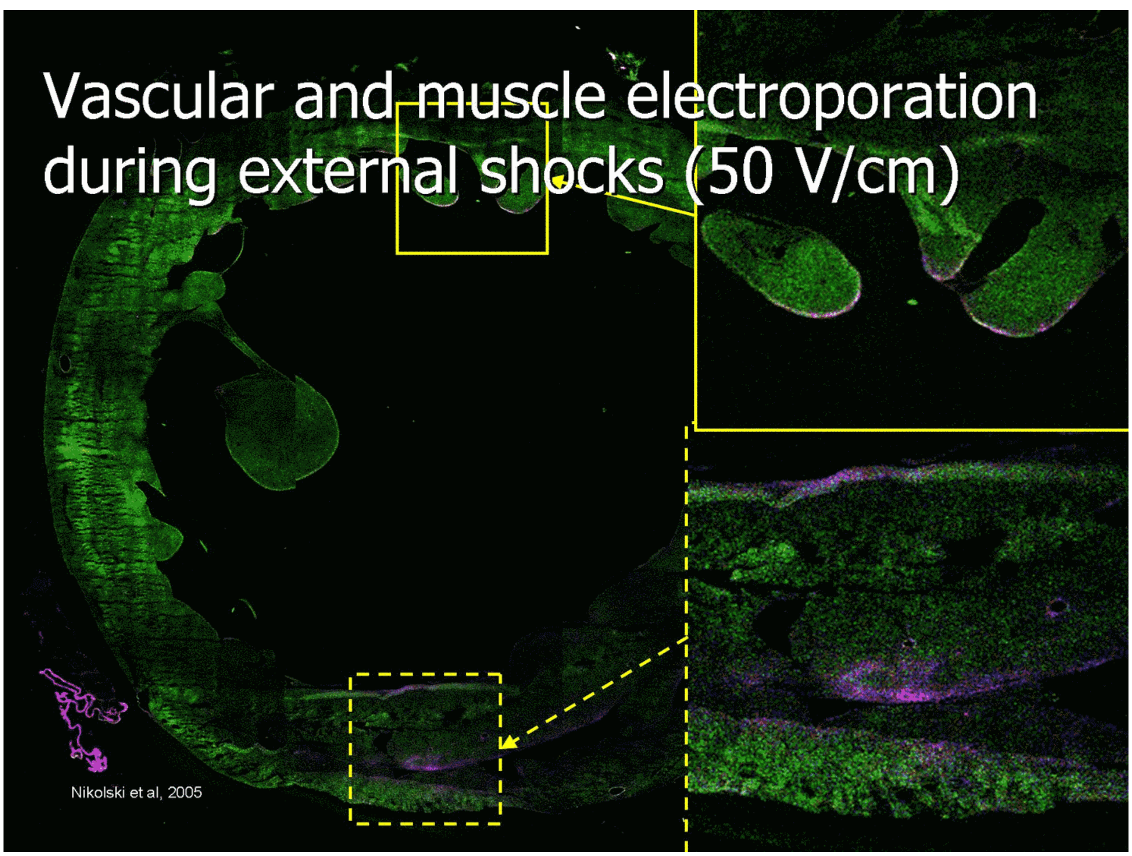
Vascular and muscle electroporation
during external shocks (50 V/cm)
Nikolski et al, 2005

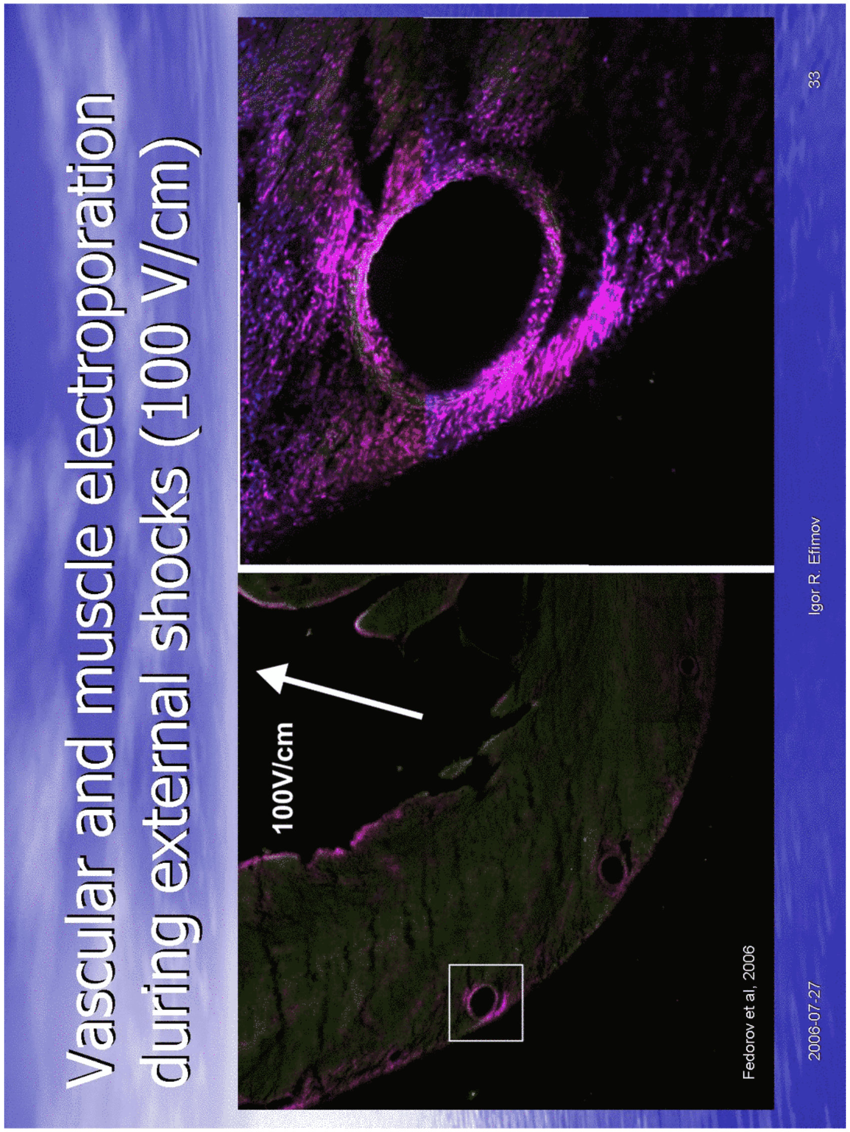
Vascular and muscle electroporation during external shocks (100 V/cm)
100V/cm
Fedorov et al, 2006
2006-07-27
Igor R. Efimov
33

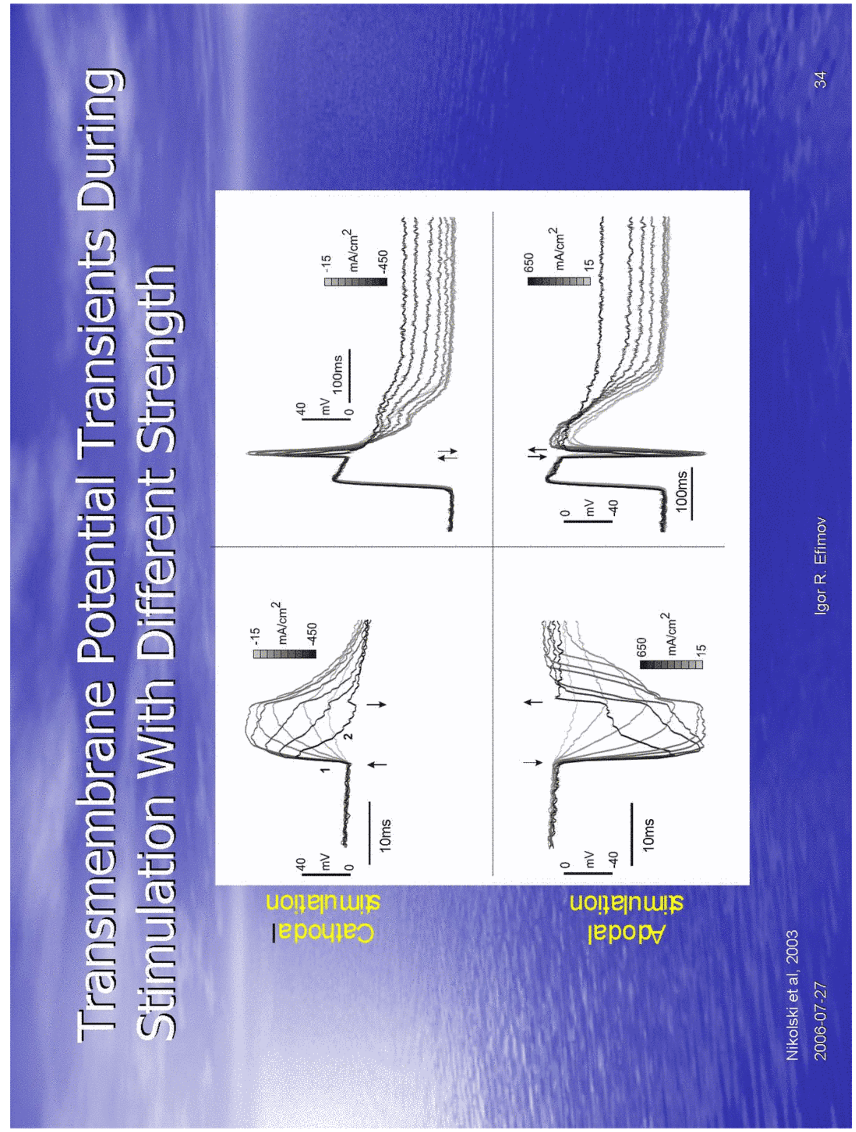
Transmembrane Potential Transients During Stimulation With Different Strength
Cathodal stimulation
Anodal stimulation
10ms
100ms
mV
mA/cm2
Nikolski et al, 2003
2006-07-27
Igor R. Efimov
34

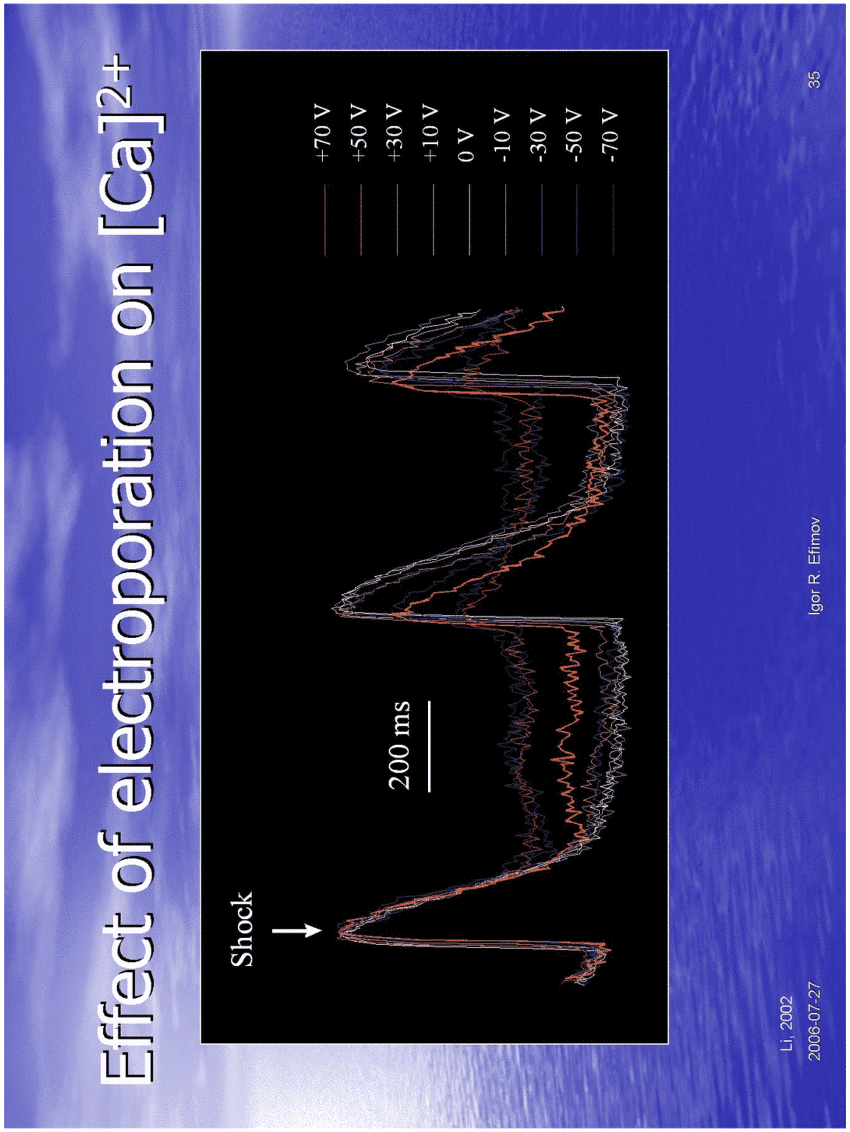
Effect of electroporation on [Ca]2+
Shock
200 ms
+70 V
+50 V
+30 V
+10 V
0 V
-10 V
-30 V
-50 V
-70 V
Li, 2002
2006-07-27
Igor R. Efimov
35

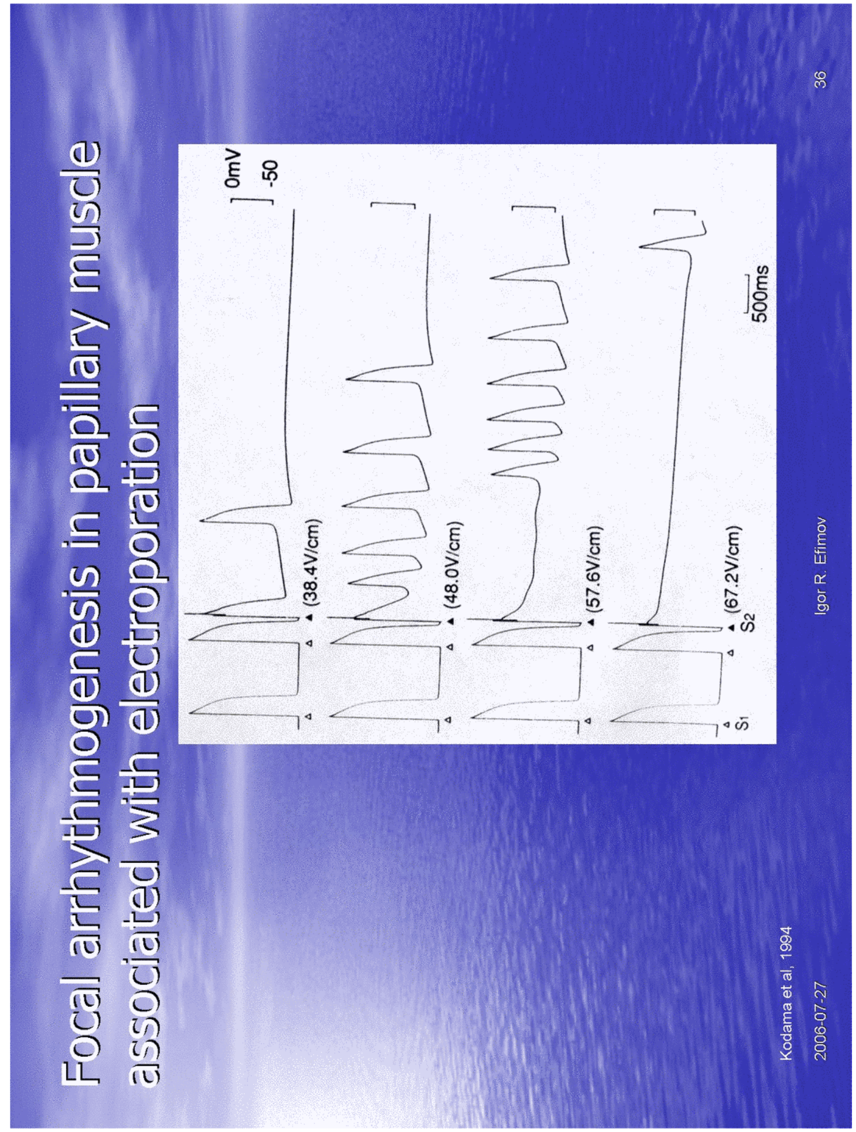
Focal arrhythmogenesis in papillary muscle associated with electroporation
0mV
-50
(38.4V/cm)
(48.0V/cm)
(57.6V/cm)
(67.2V/cm)
S1
S2
500ms
Kodama et al, 1994
2006-07-27
Igor R. Efimov
36

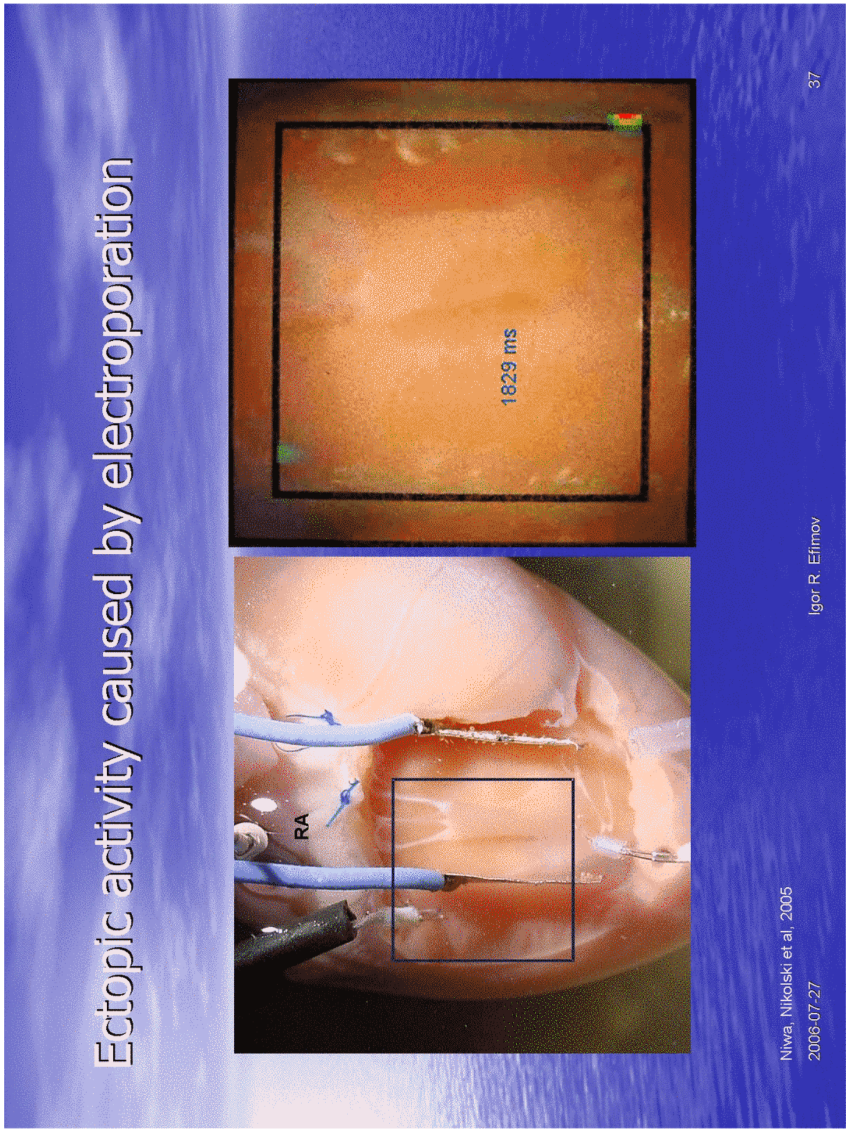
Ectopic activity caused by electroporation
RA
1829 ms
Niwa, Nikolski et al, 2005
2006-07-27
Igor R. Efimov
37

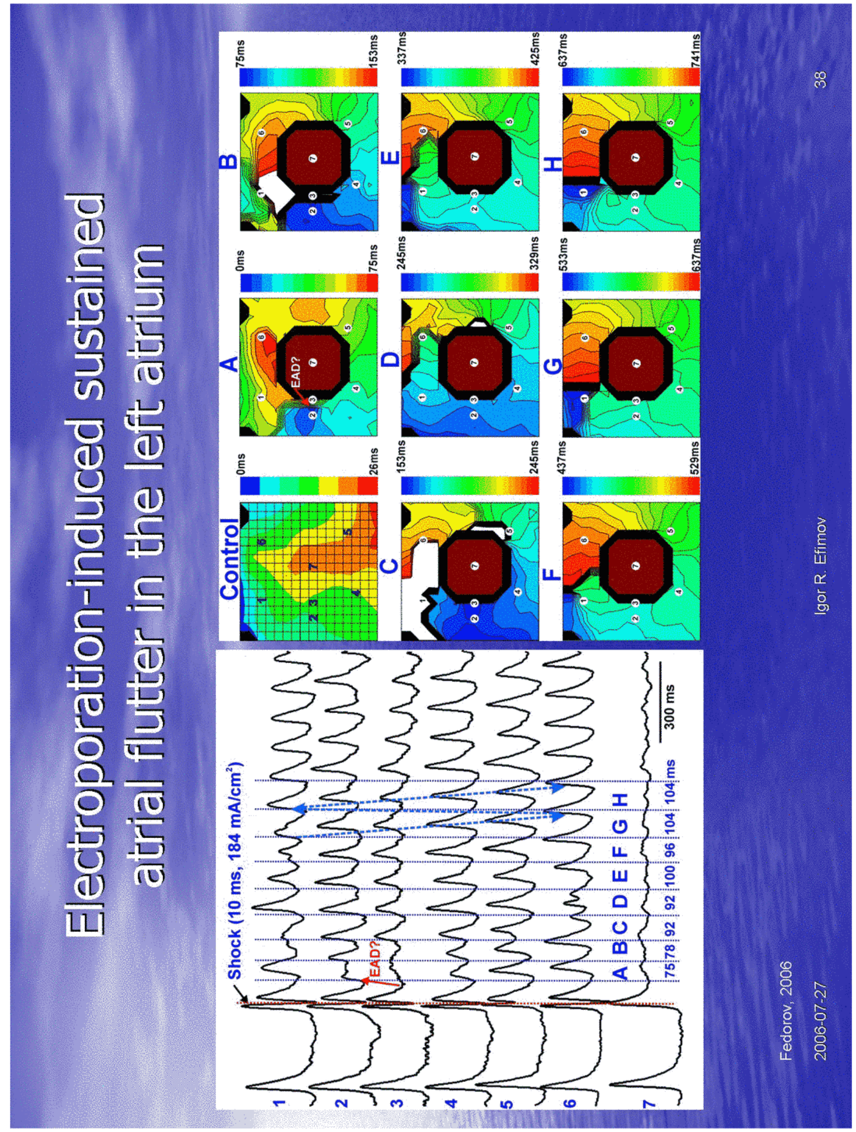
Electroporation-induced sustained atrial flutter in the left atrium
Shock (10 ms, 184 mA/cm²)
EAD?
A B C D E F G H
75 78 92 92 100 96 104 104 ms
300 ms
Control
A
B
C
D
E
F
G
H
Fedorov, 2006
2006-07-27
Igor R. Efimov
38

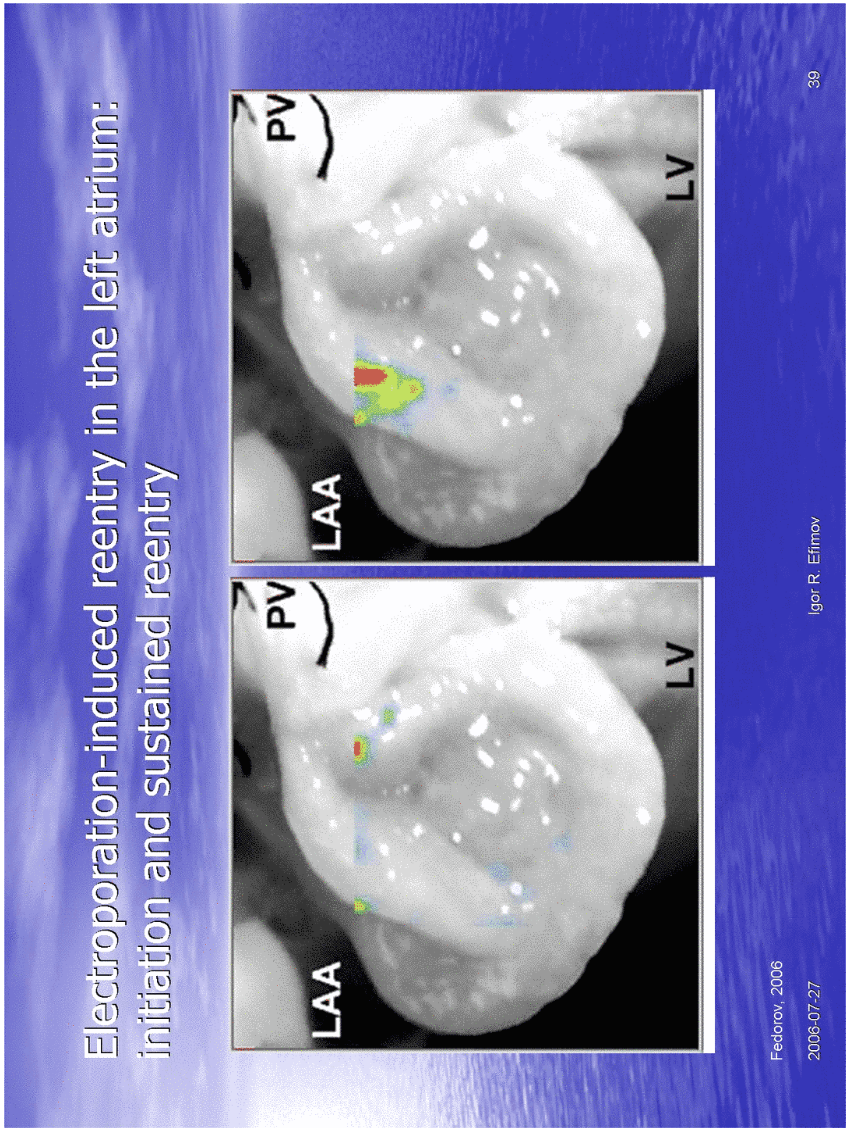
Electroporation-induced reentry in the left atrium:
initiation and sustained reentry
PV
LV
LAA
PV
LV
LAA
Fedorov, 2006
2006-07-27
Igor R. Efimov
39


Clinical evidence of post-shock
slowing of conduction
2006-07-27
Igor R. Efimov
40

Post-shock delay in recovery of normal ventricular conduction (56 pts): ventricular conduction slowed in 87.3%

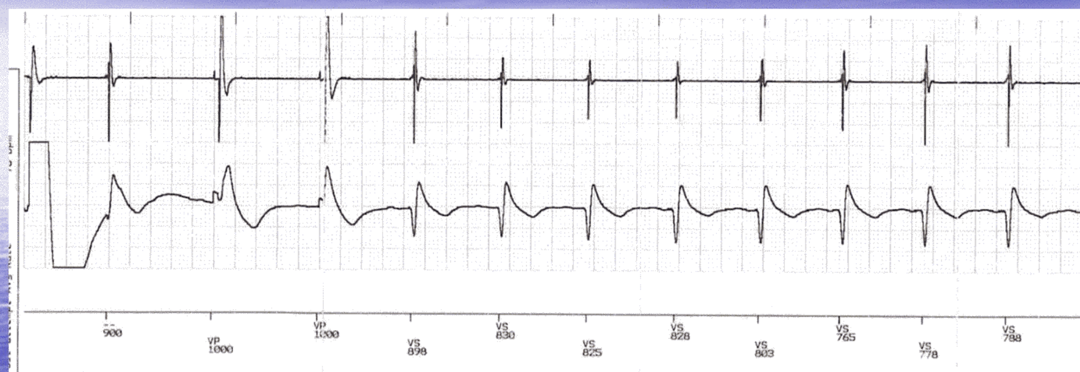

Typical post-shock ICD recording, found in 87.3% patients. Near-field (top) and far-field (bottom) electrograms recorded during 10 seconds starting immediately after 21J ICD shock. Widening of intracardiac EGM was observed in 87.3%, failure of conduction recovery was observed in 40% of cases.

Post-shock Conduction Slowing: Sinus Rhythm (A) vs Pacing (B)

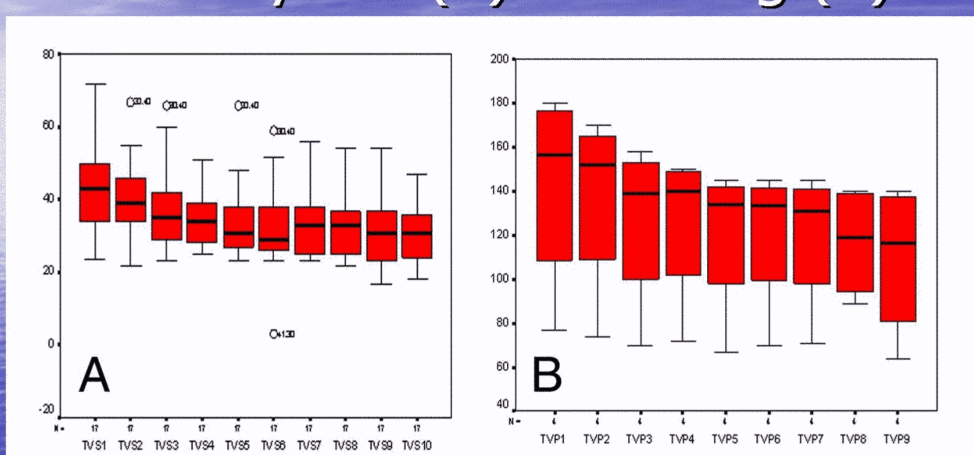

The mean of the initial intracardiac EGM in ventricular-sensed (A) and ventricular-paced beats during 10 seconds after ICD shock was significantly higher than in 10 control beats: 34.7±12.9 vs 28.1±10.9 ms ($p<0.0001$) and 136.6±51.6 vs 114.1±28.2 ms ($p=0.039$), respectively.

Tereshchenko, 2006


5. Low-voltage defibrillation: structural basis of arrhythmia and defibrillation
2006-07-27
Igor R. Efimov
43

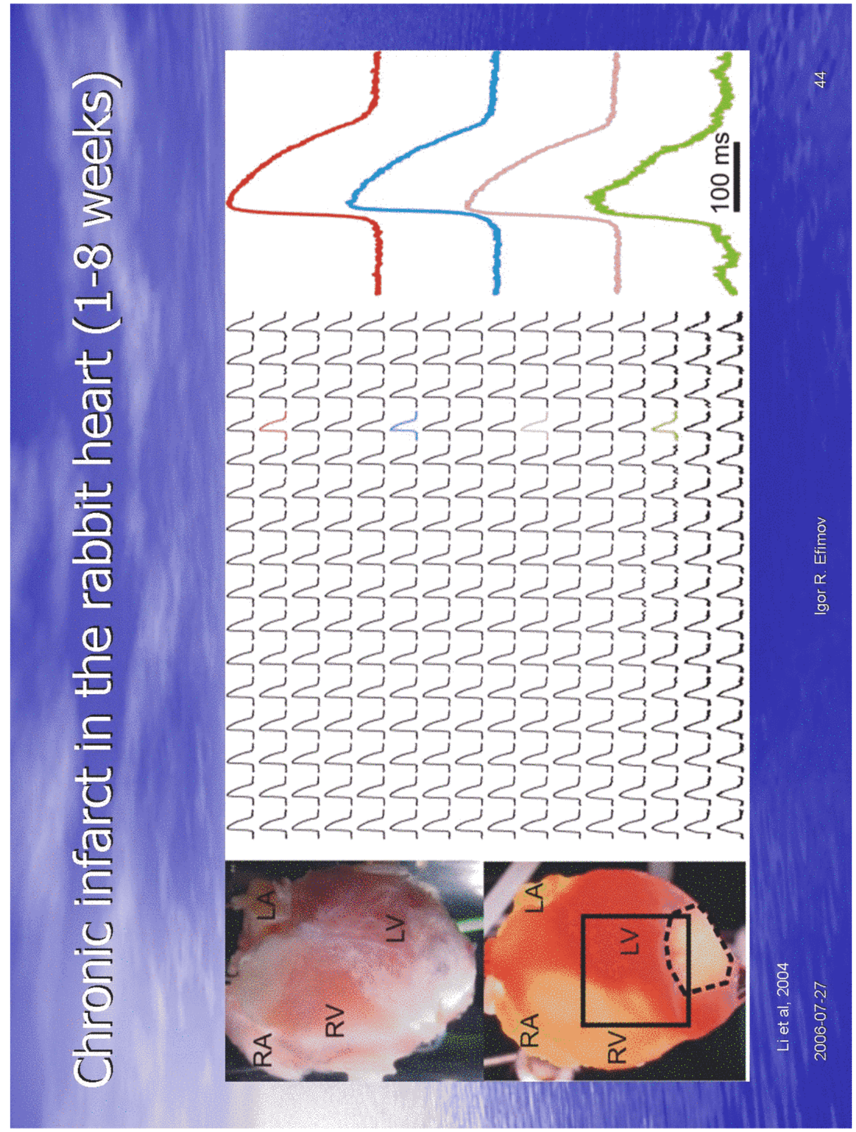
Chronic infarct in the rabbit heart (1-8 weeks)
RA
RV
LV
LA
100 ms
Li et al, 2004
2006-07-27
Igor R. Efimov
44

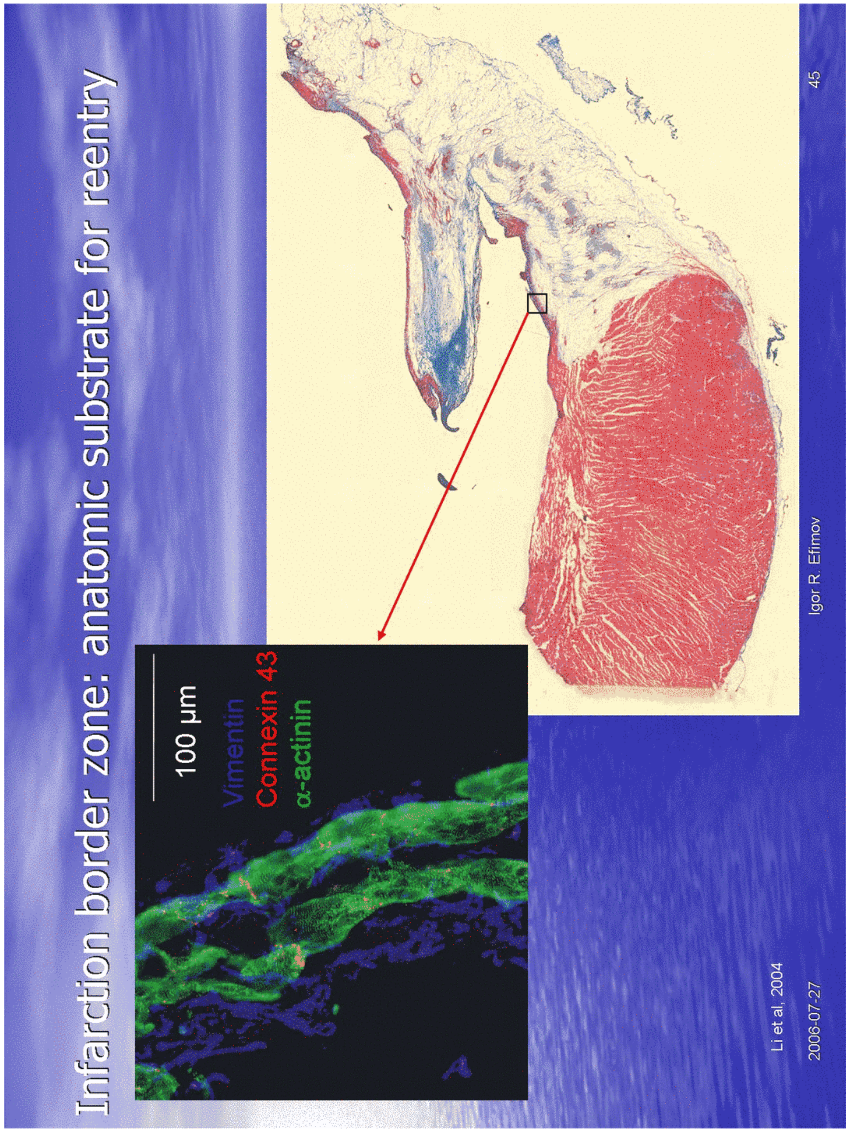
Infarction border zone: anatomic substrate for reentry
100 µm
Vimentin
Connexin 43
α-actinin
Li et al, 2004
2006-07-27
Igor R. Efimov
45

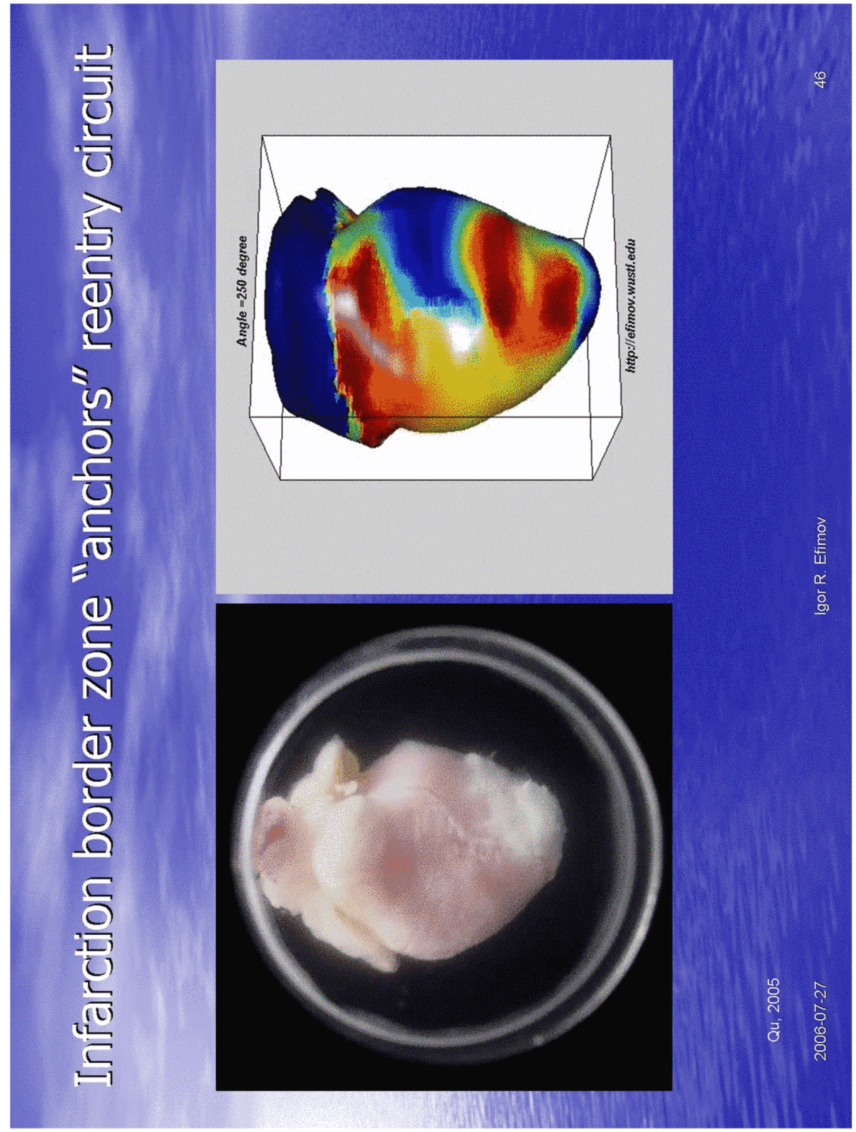
Infarction border zone "anchors" reentry circuit
Angle =250 degree
http://efimov.wustl.edu
Qu, 2005
2006-07-27
Igor R. Efimov
46

Biophysical mechanism

- Reentry "pins" to a scar or other resistive heterogeneity in the myocardium
- Applied electric field produces maximum effect (virtual electrode polarization) at the scar or other heterogeneity area due to activating function/VEP effect

2006-07-27 Igor R. Efimov 47

Reentry "unpinning" by a low-energy shock

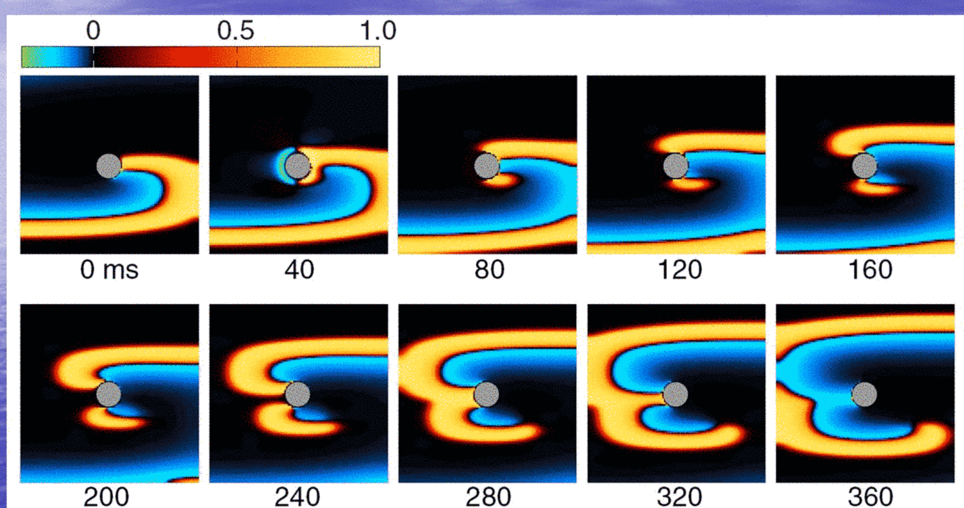

Takagi et al, 2004

2006-07-27 Igor R. Efimov 48

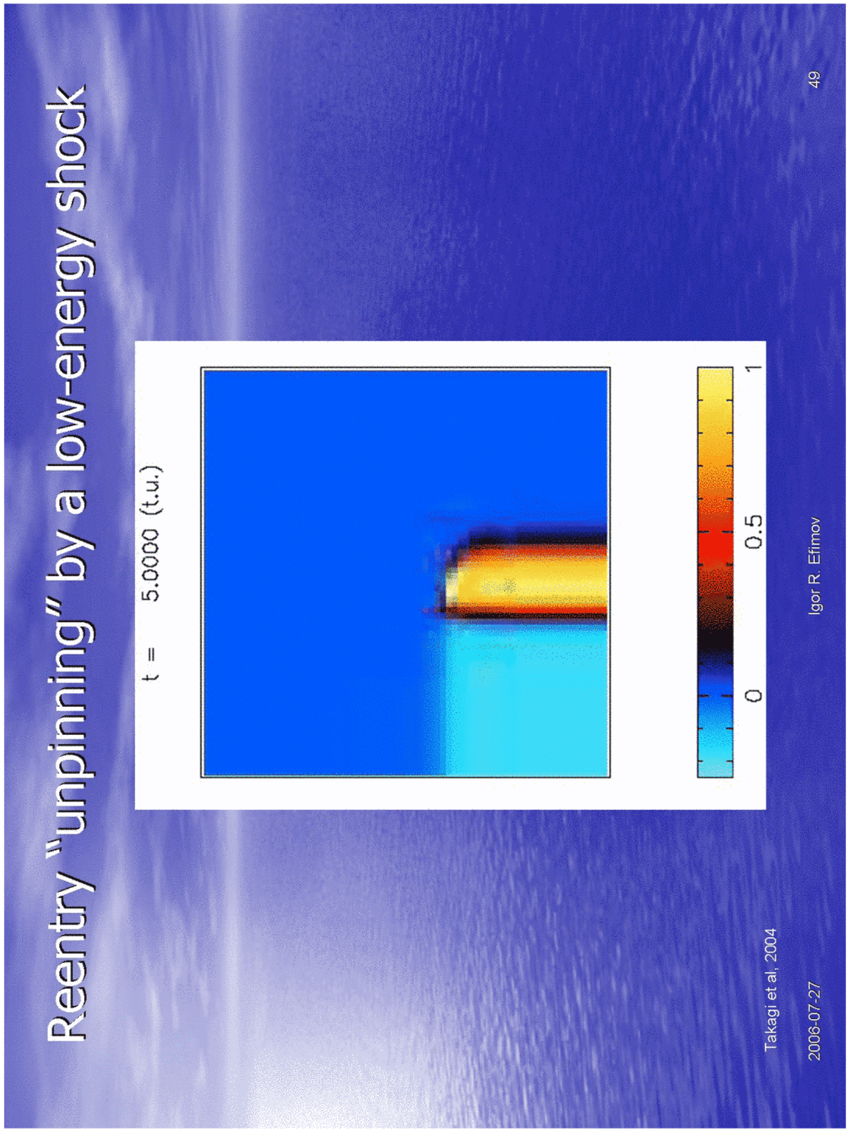
Reentry “unpinning” by a low-energy shock
t = 5.0000 (t.u.)
0
0.5
1
Takagi et al, 2004
2006-07-27
Igor R. Efimov
49

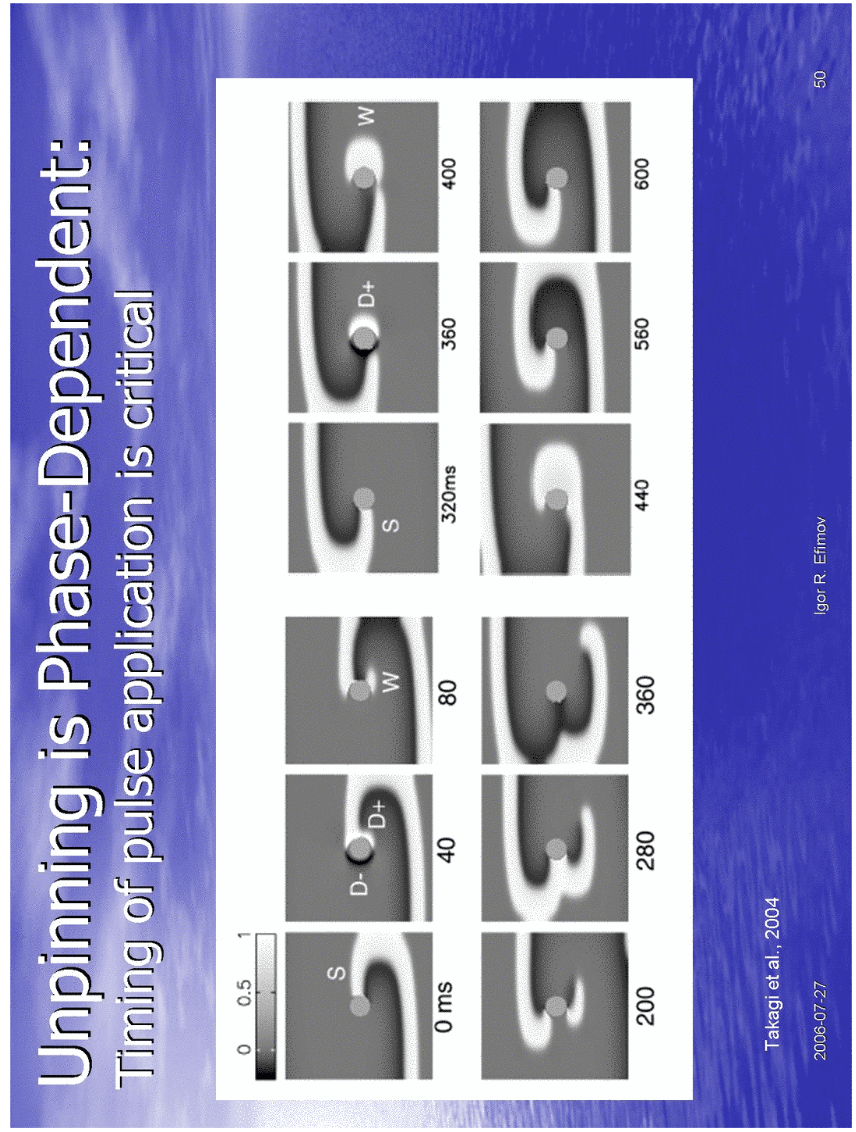
Unpinning is Phase-Dependent:
Timing of pulse application is critical
0
0.5
1
S
0 ms
D-
D+
40
W
80
200
280
360
S
320ms
D+
360
W
400
440
560
600
Takagi et al., 2004
2006-07-27
Igor R. Efimov
50

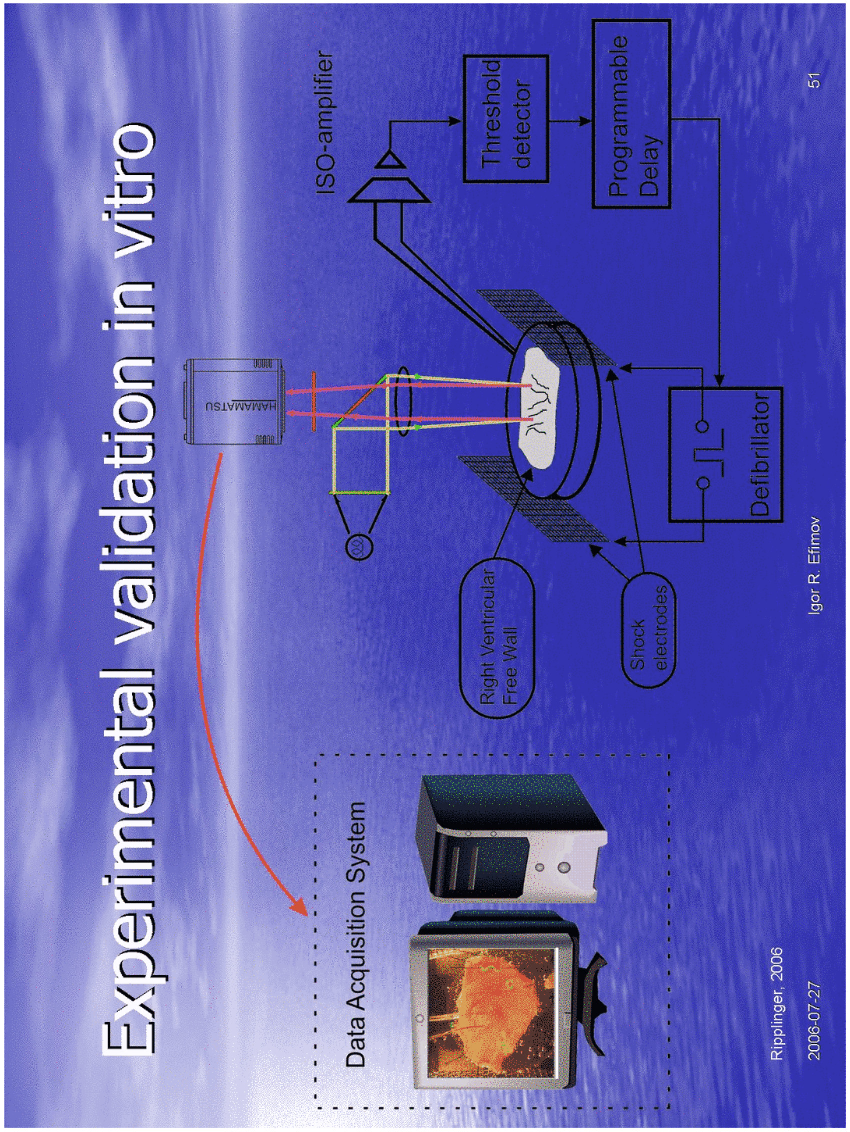
Experimental validation in vitro
Data Acquisition System
HAMAMATSU
ISO-amplifier
Threshold detector
Programmable Delay
Right Ventricular Free Wall
Shock electrodes
Defibrillator
Ripplinger, 2006
2006-07-27
Igor R. Efimov
51

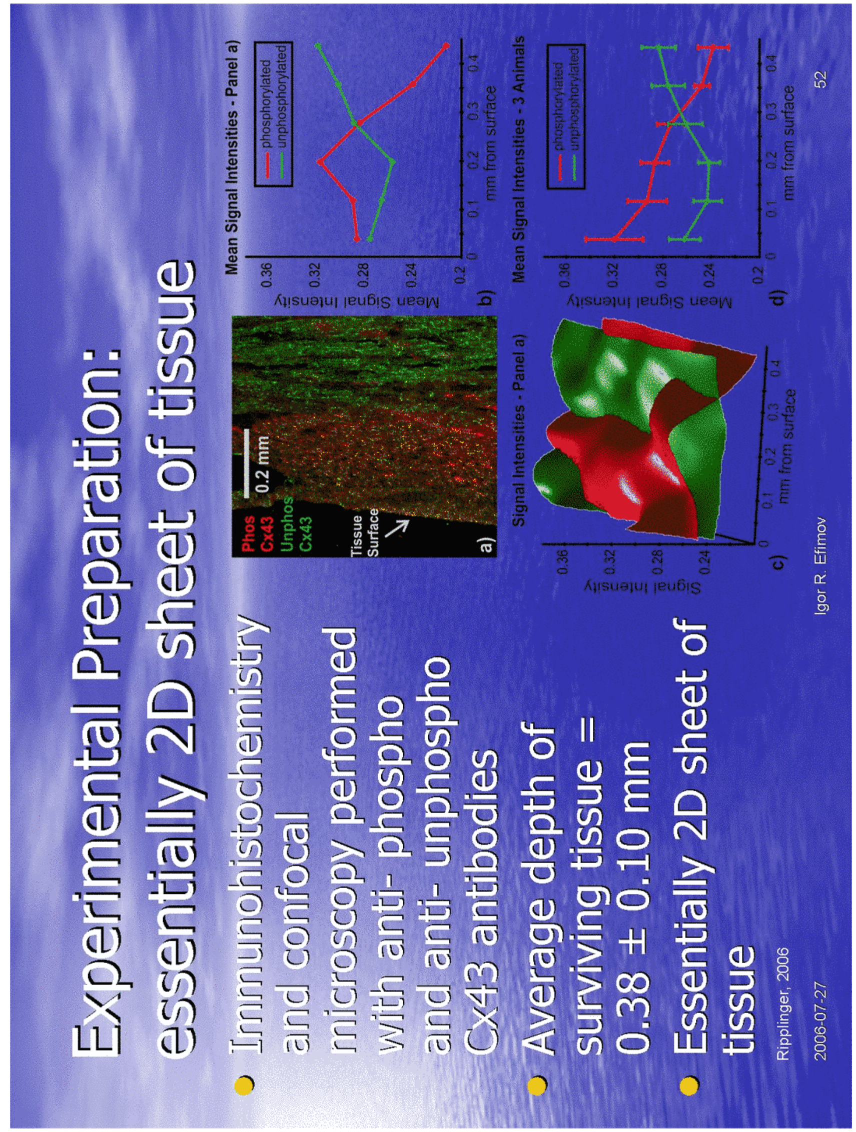
Experimental Preparation: essentially 2D sheet of tissue
Immunohistochemistry and confocal microscopy performed with anti- phospho and anti- unphospho Cx43 antibodies
Average depth of surviving tissue = 0.38 ± 0.10 mm
Essentially 2D sheet of tissue
Phos Cx43
Unphos Cx43
0.2 mm
Tissue Surface
a)
Mean Signal Intensities - Panel a)
phosphorylated
unphosphorylated
Mean Signal Intensity
mm from surface
b)
Signal Intensities - Panel a)
Signal Intensity
mm from surface
c)
Mean Signal Intensities - 3 Animals
phosphorylated
unphosphorylated
Mean Signal Intensity
mm from surface
d)
Ripplinger, 2006
2006-07-27
Igor R. Efimov
52

Connexin 43 dephosphorylation and cell uncoupling in the superfused RV preparation: acute model of infarct border zone, which "pins" reentry

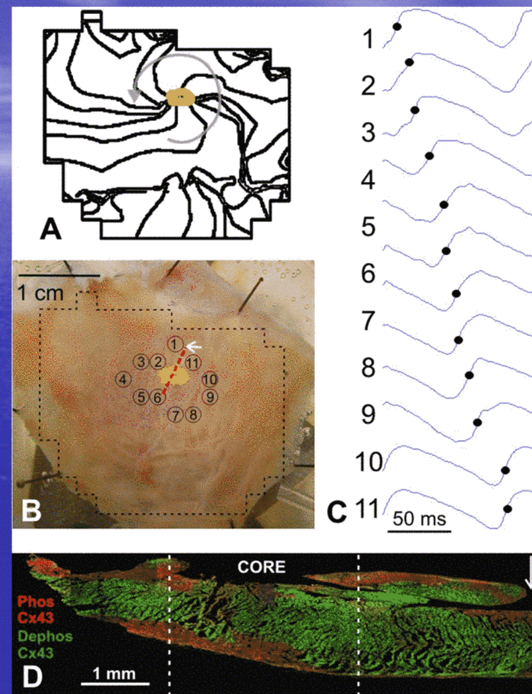

Ripplinger et al., 2006

VEP and reentry core

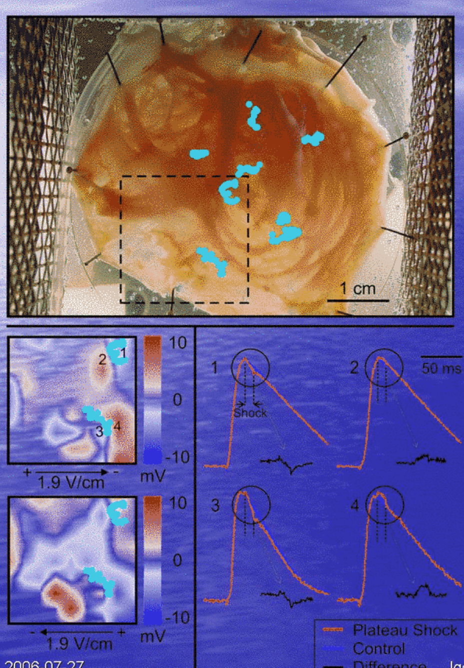

- Reentry cores correspond to areas of adjacent positive and negative polarization, indicating underlying anatomical or functional heterogeneity
- Within 2 mm radius of cores, average ± VEP was 3.6 ± 0.5 mV and -3.5 ± 0.6 mV
- Positive polarization necessary to unpin reentry

Ripplinger, 2006

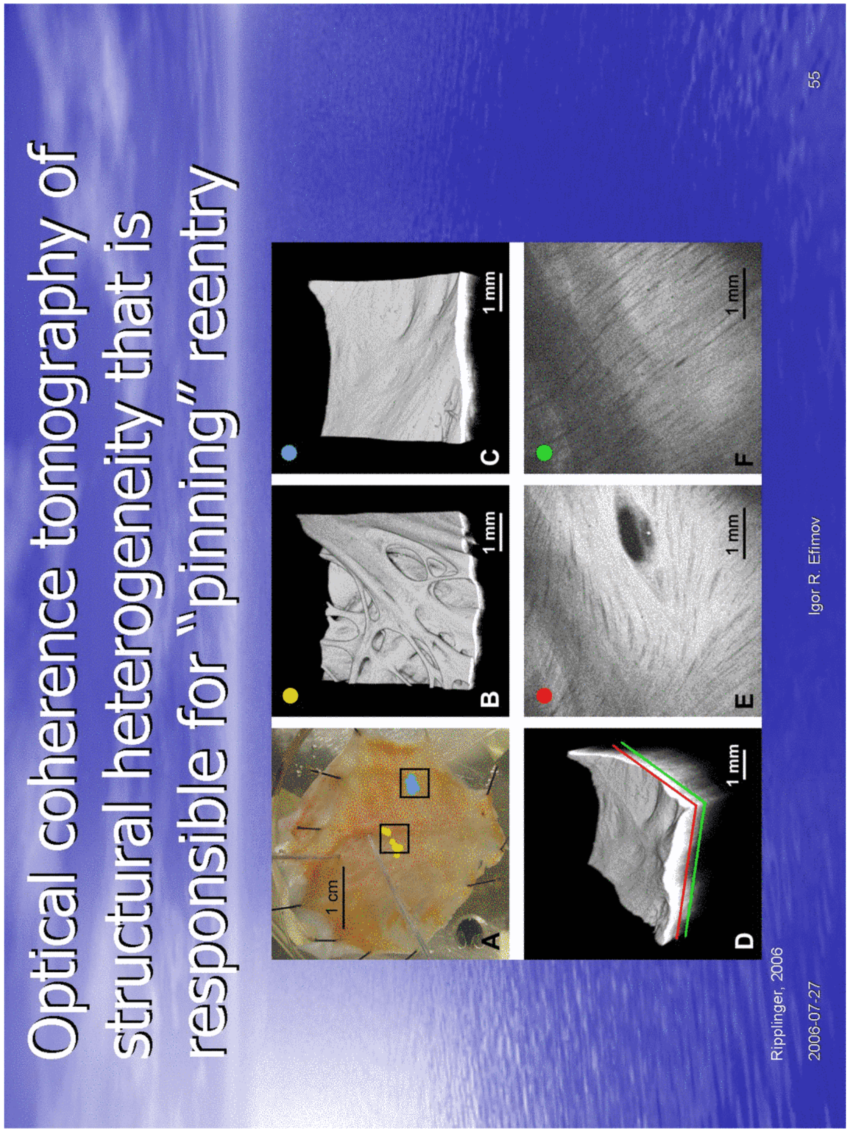
Optical coherence tomography of structural heterogeneity that is responsible for "pinning" reentry
Ripplinger, 2006
2006-07-27
Igor R. Efimov
55

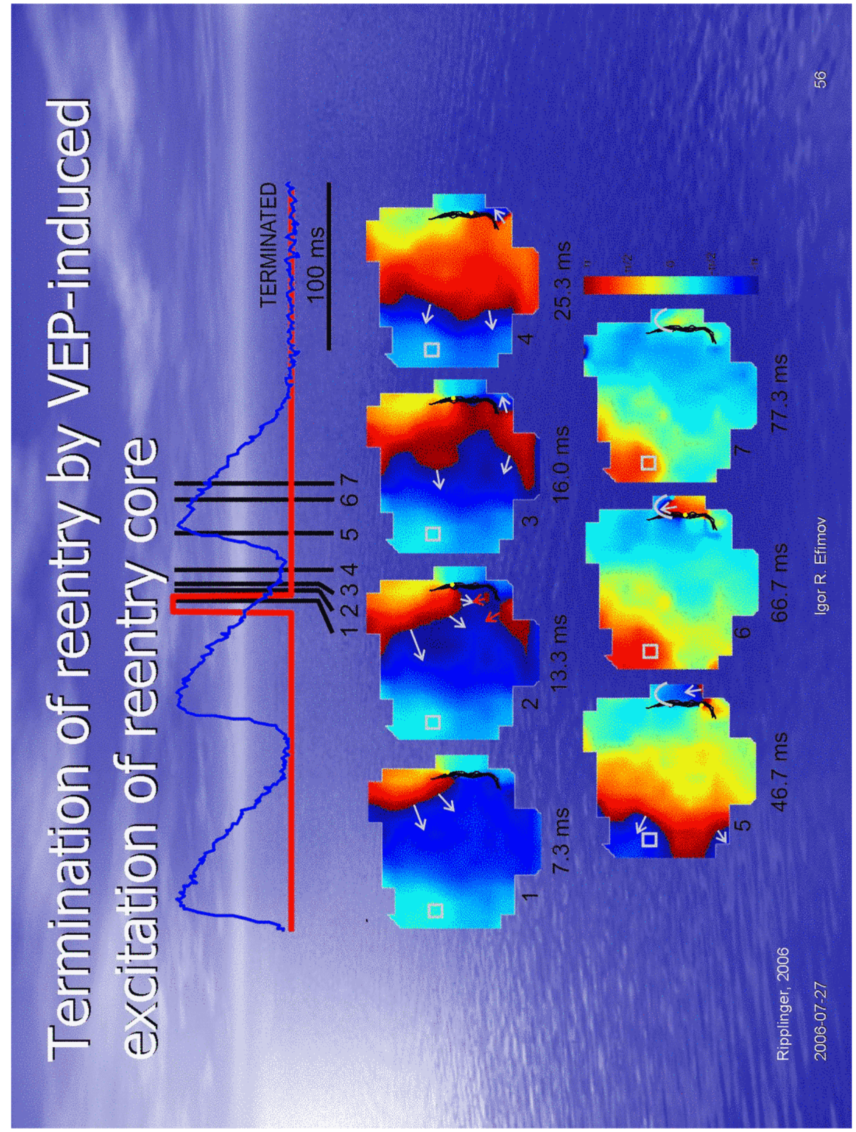
Termination of reentry by VEP-induced excitation of reentry core
TERMINATED
100 ms
7.3 ms
13.3 ms
16.0 ms
25.3 ms
46.7 ms
66.7 ms
77.3 ms
Ripplinger, 2006
2006-07-27
Igor R. Efimov
56

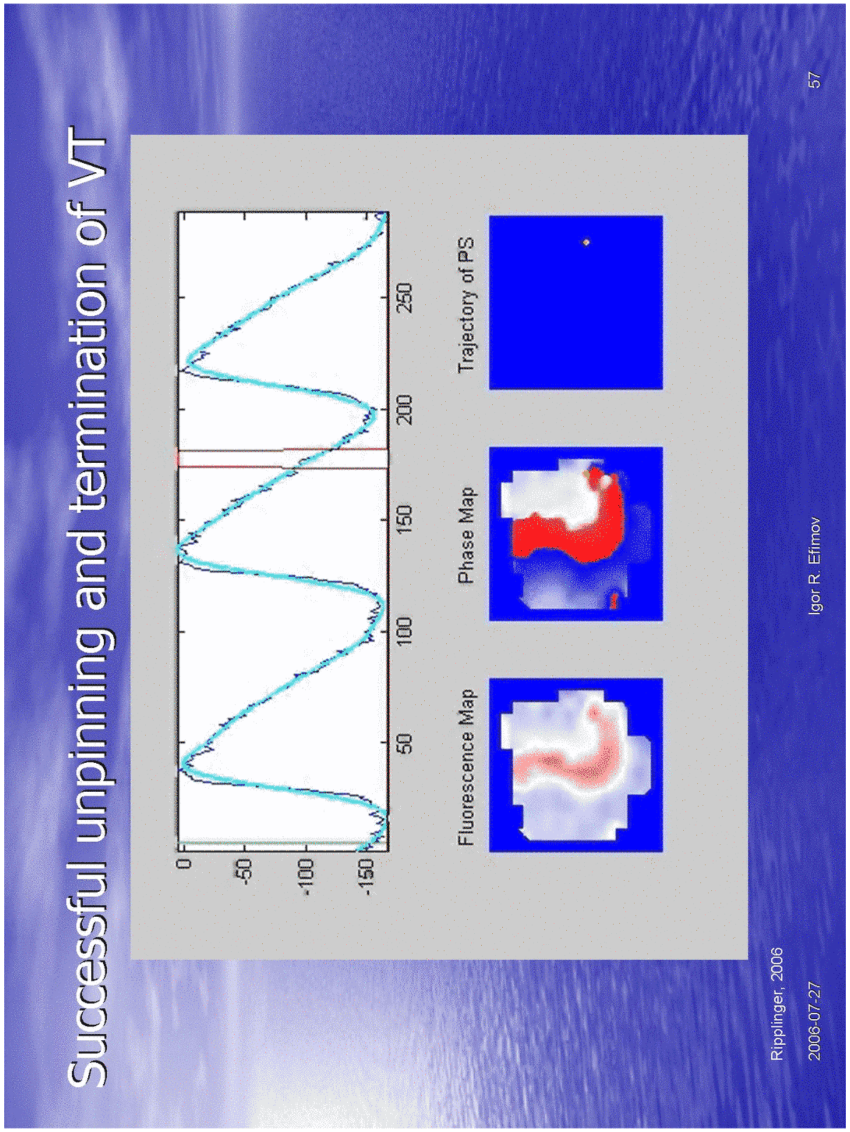
Successful unpinning and termination of VT
0
-50
-100
-150
50
100
150
200
250
Fluorescence Map
Phase Map
Trajectory of PS
Ripplinger, 2006
2006-07-27
Igor R. Efimov
57

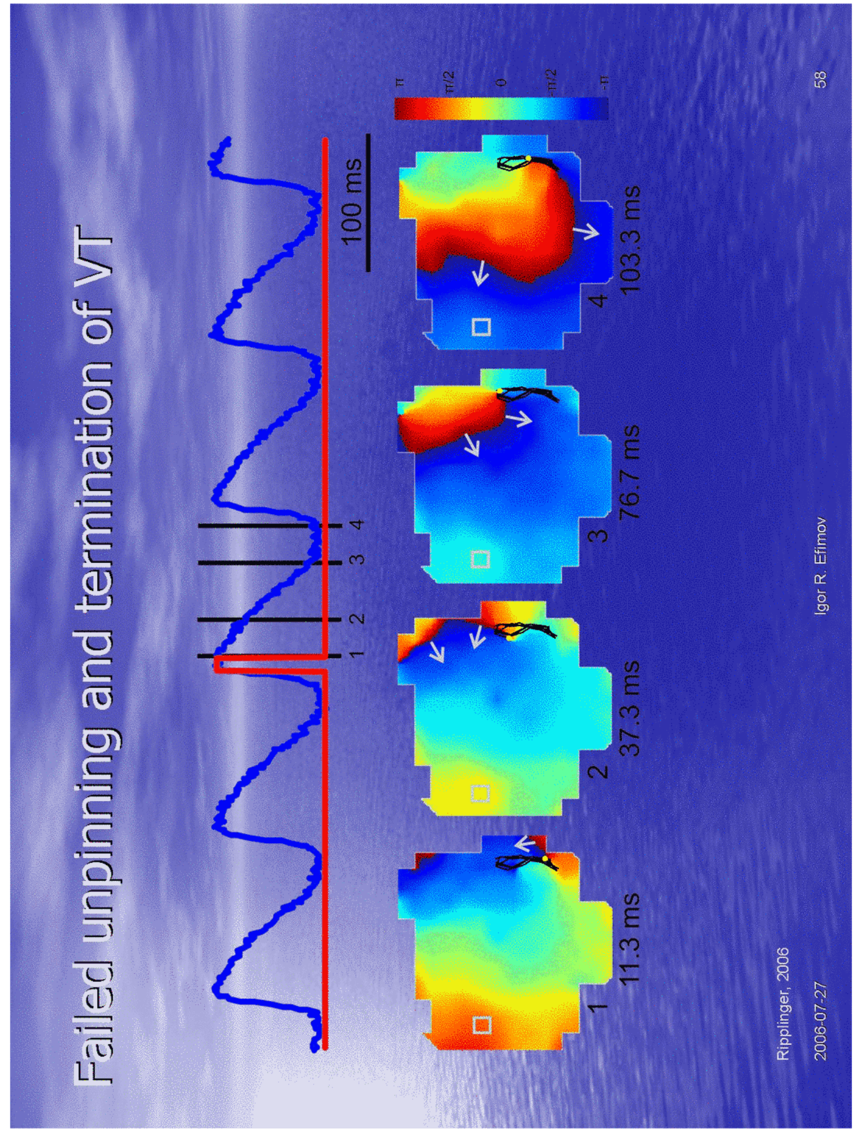
Failed unpinning and termination of VT
100 ms
1
2
3
4
π
π/2
0
-π/2
-π
1 11.3 ms
2 37.3 ms
3 76.7 ms
4 103.3 ms
Ripplinger, 2006
2006-07-27
Igor R. Efimov
58

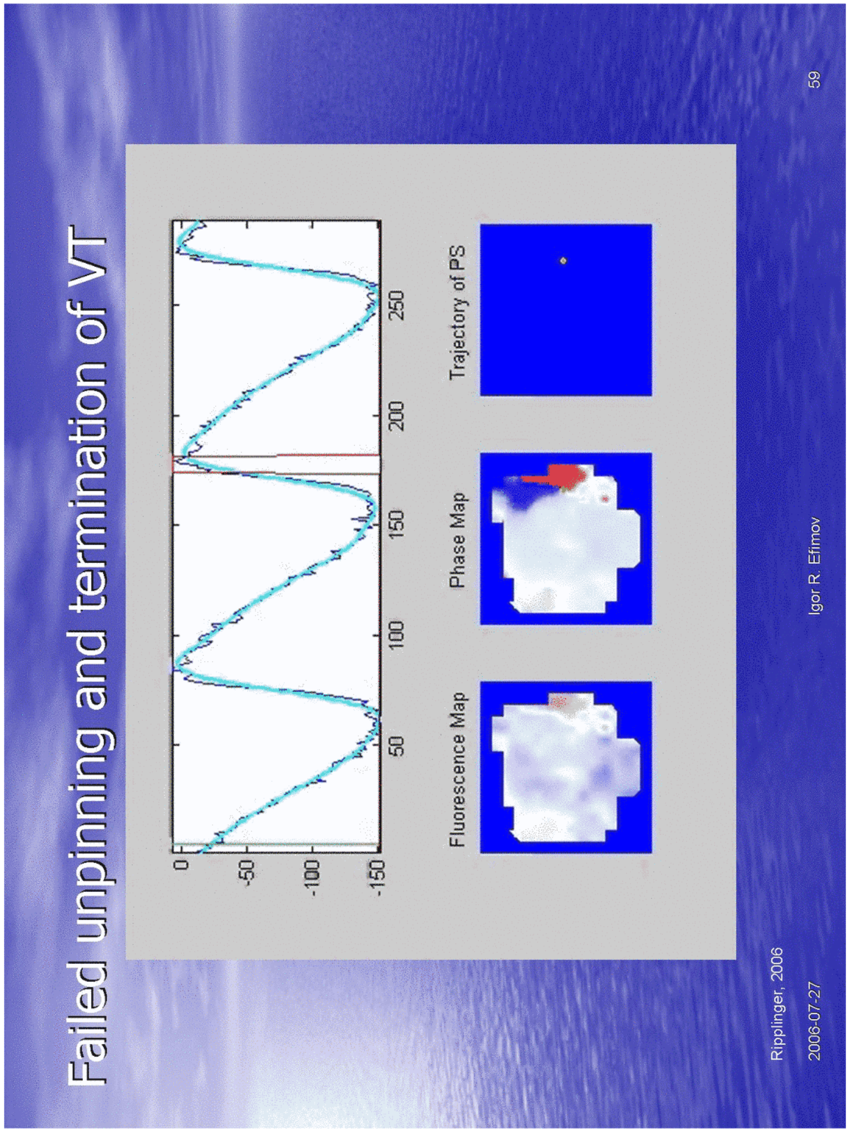

Failed unpinning and termination of VT
0
-50
-100
-150
50
100
150
200
250
Fluorescence Map
Phase Map
Trajectory of PS
Ripplinger, 2006
2006-07-27
Igor R. Efimov
59

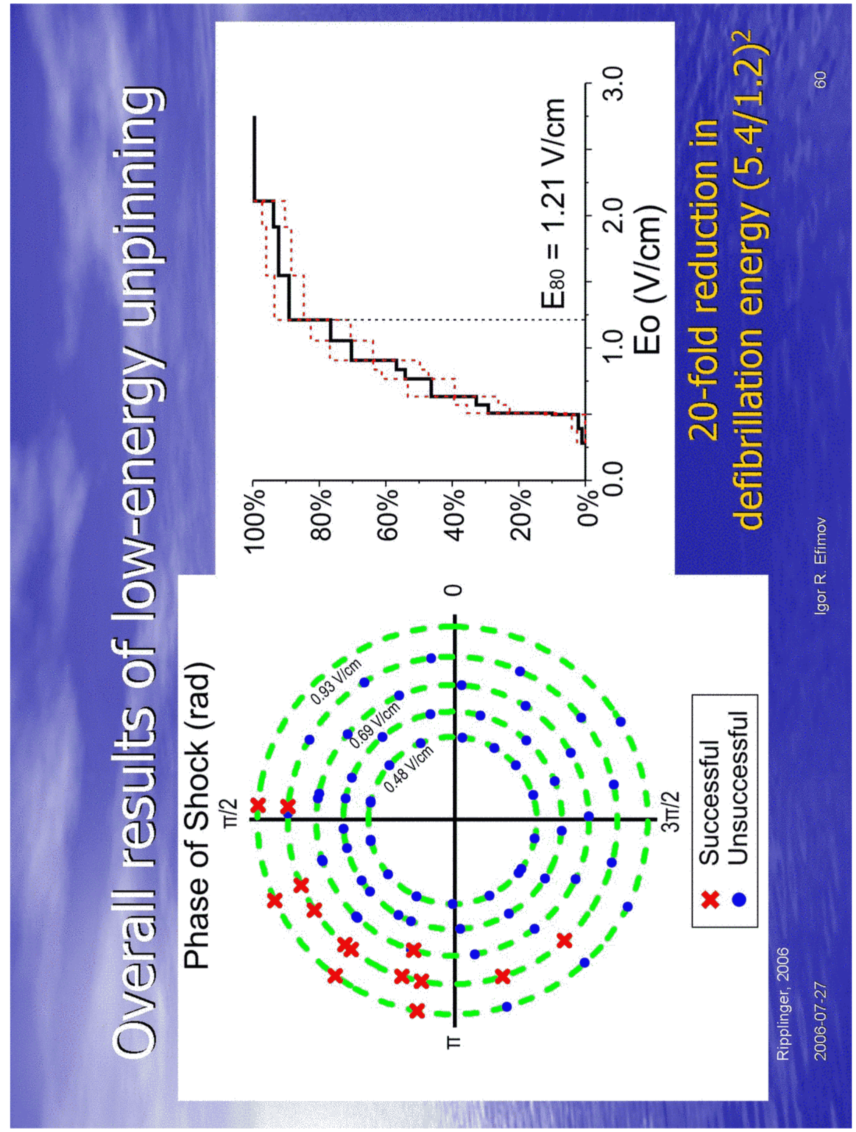

Overall results of low-energy unpinning
Phase of Shock (rad)
π/2
0
π
3π/2
0.93 V/cm
0.69 V/cm
0.48 V/cm
Successful
Unsuccessful
100%
80%
60%
40%
20%
0%
0.0
1.0
2.0
3.0
Eo (V/cm)
E_{80} = 1.21 V/cm
20-fold reduction in
defibrillation energy $(5.4/1.2)^2$
Ripplinger, 2006
2006-07-27
Igor R. Efimov
60

6. Low voltage defibrillation in the 4-day canine model of infarction and VT

Position of electrodes

Heart of open chest canine #1 (male, 18.5 kg)

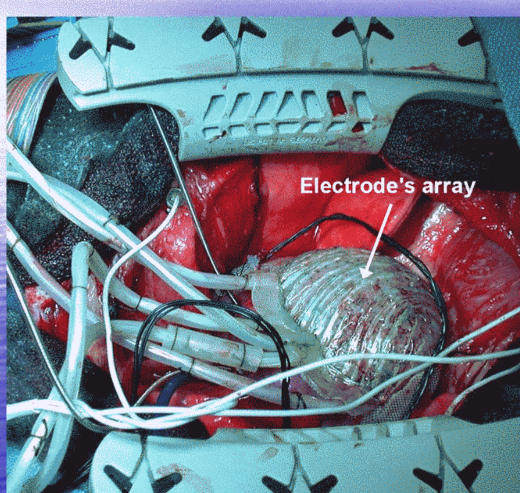

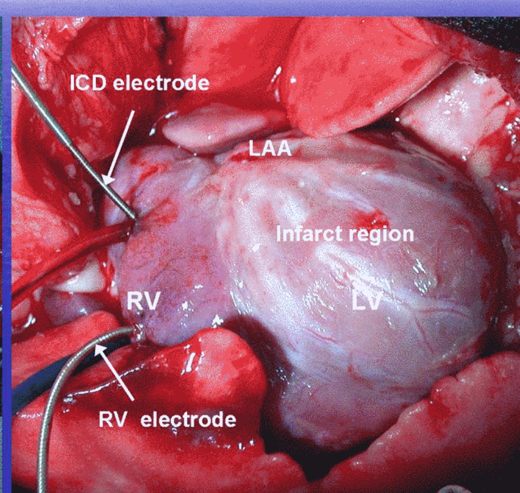

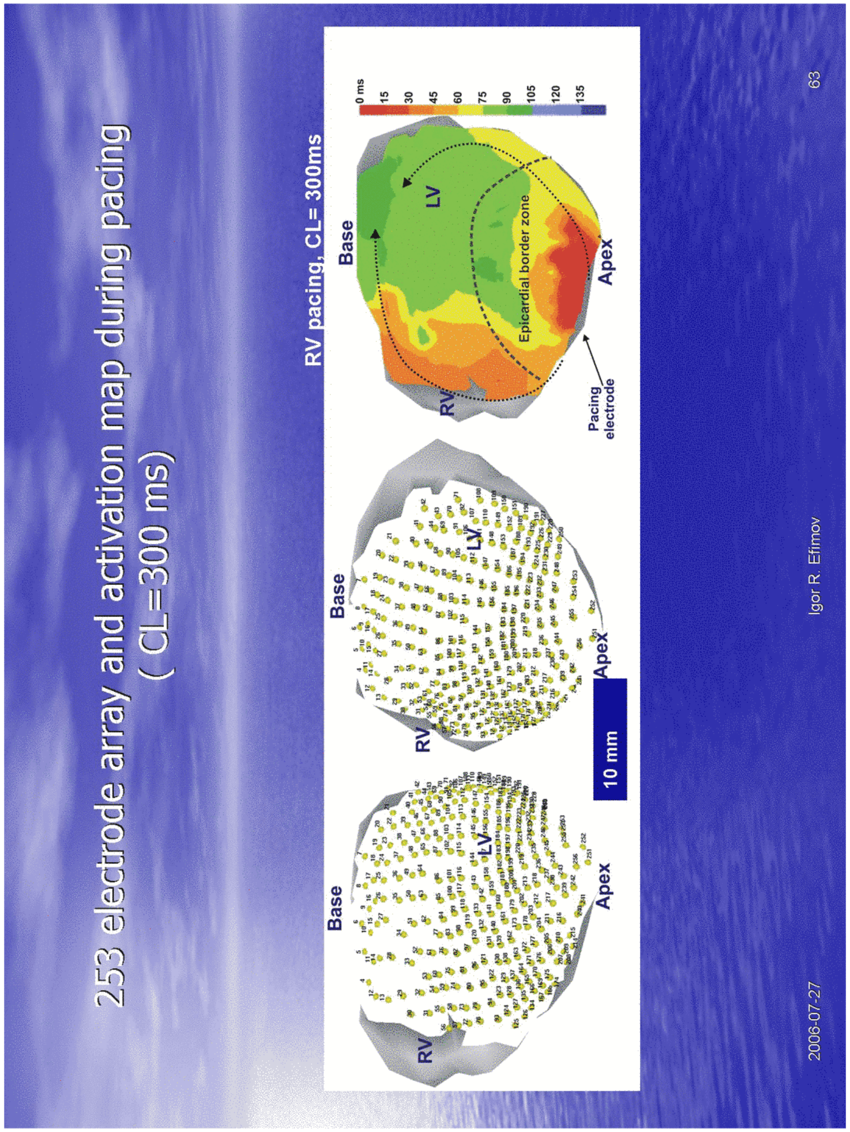
253 electrode array and activation map during pacing
(CL=300 ms)
RV pacing, CL= 300ms
Base
LV
RV
Apex
Base
LV
RV
Apex
10 mm
Base
LV
RV
Apex
Epicardial border zone
Pacing electrode
0 ms 15 30 45 60 75 90 105 120 135
2006-07-27
Igor R. Efimov
63

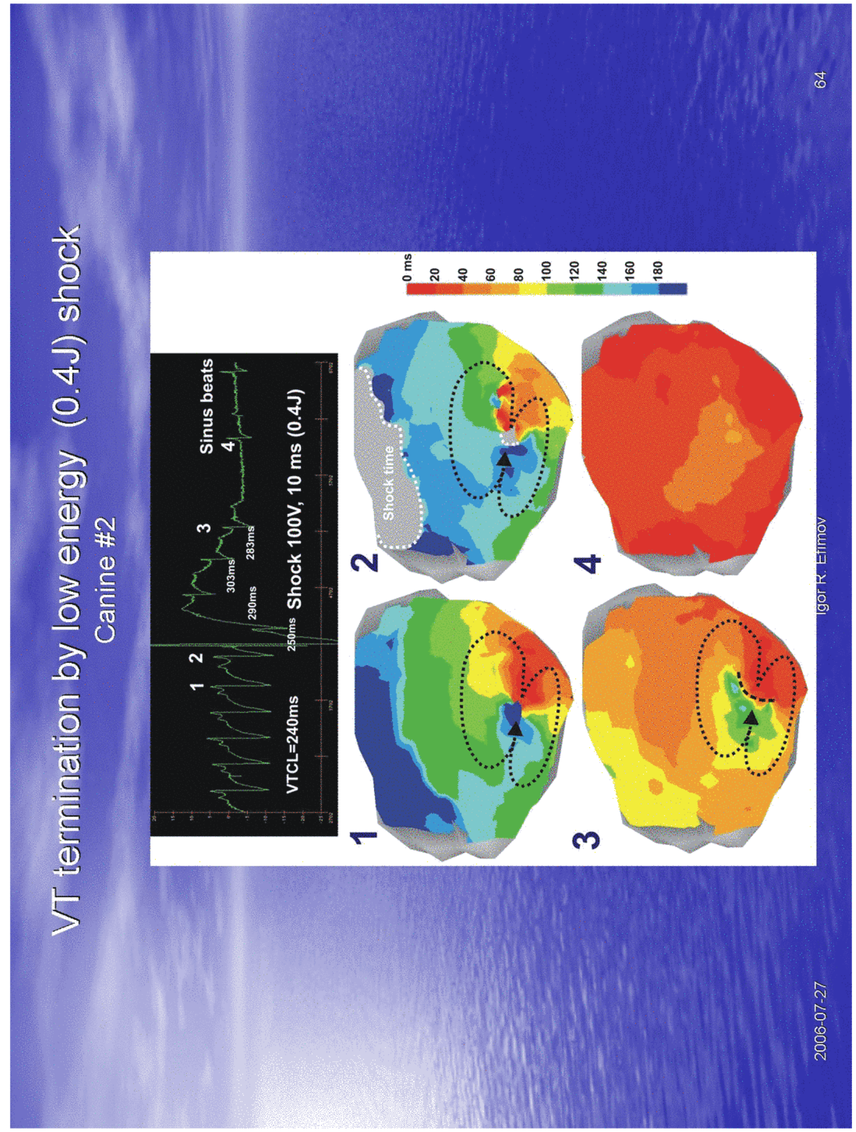
VT termination by low energy (0.4J) shock
Canine #2
1 2 3 4
Sinus beats
VTCL=240ms
250ms
290ms
303ms
283ms
Shock 100V, 10 ms (0.4J)
Shock time
0 ms 20 40 60 80 100 120 140 160 180
1
2
3
4
2006-07-27
Igor R. Efimov
64

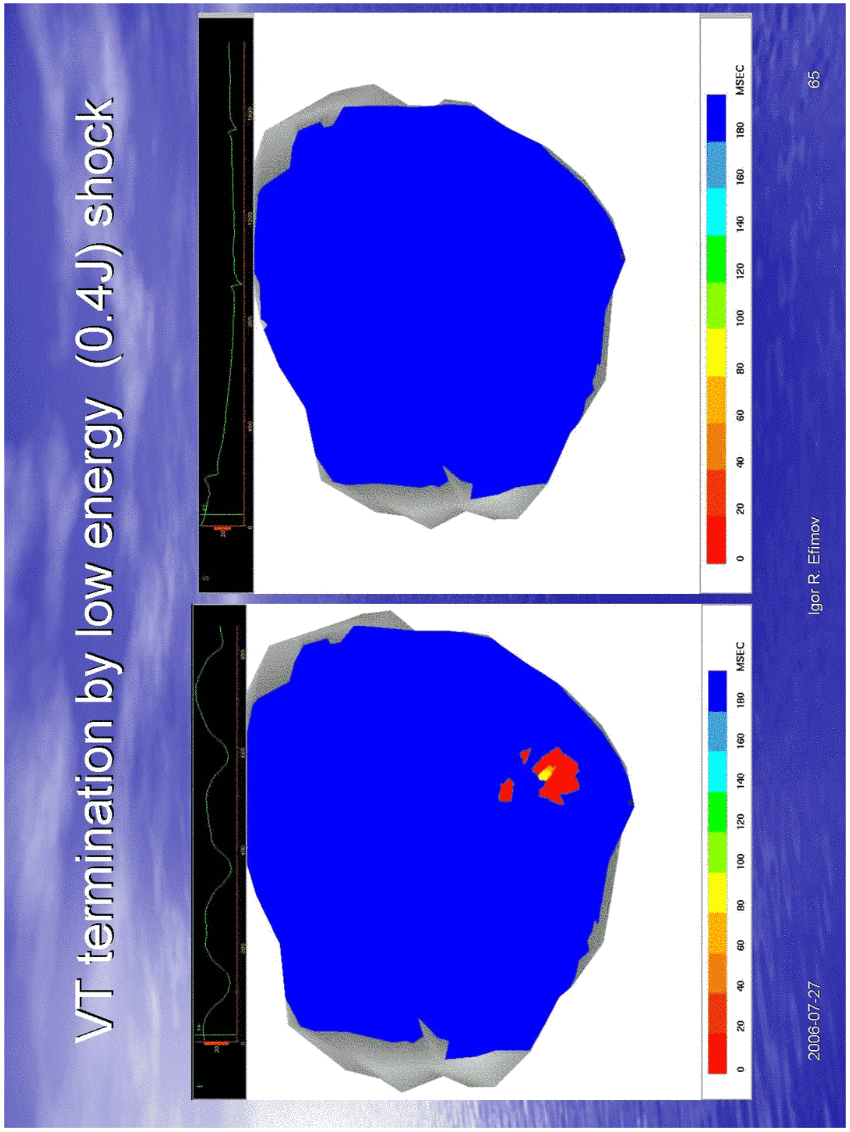
VT termination by low energy (0.4J) shock
MSEC
Igor R. Efimov
2006-07-27
65

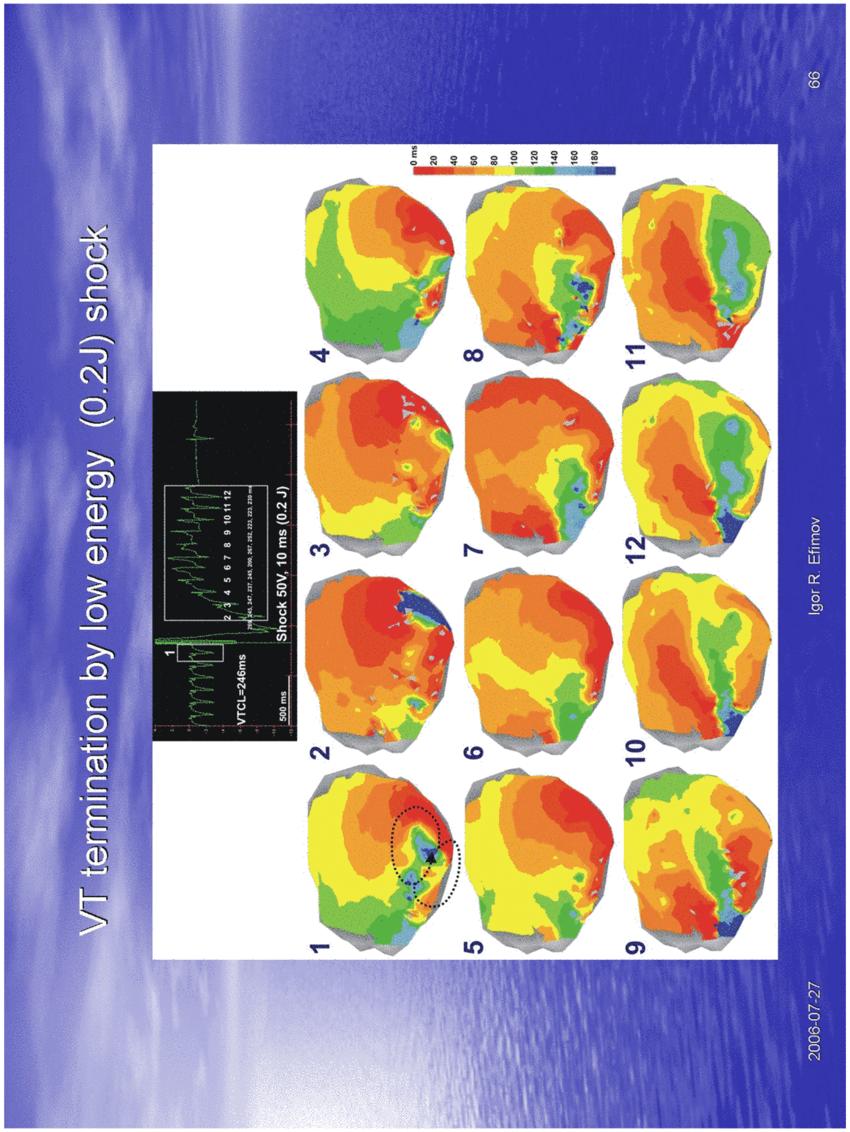
VT termination by low energy (0.2J) shock
VTCL=246ms
Shock 50V, 10 ms (0.2 J)
500 ms
1
2
3
4
5
6
7
8
9
10
11
12
Igor R. Efimov
2006-07-27
66

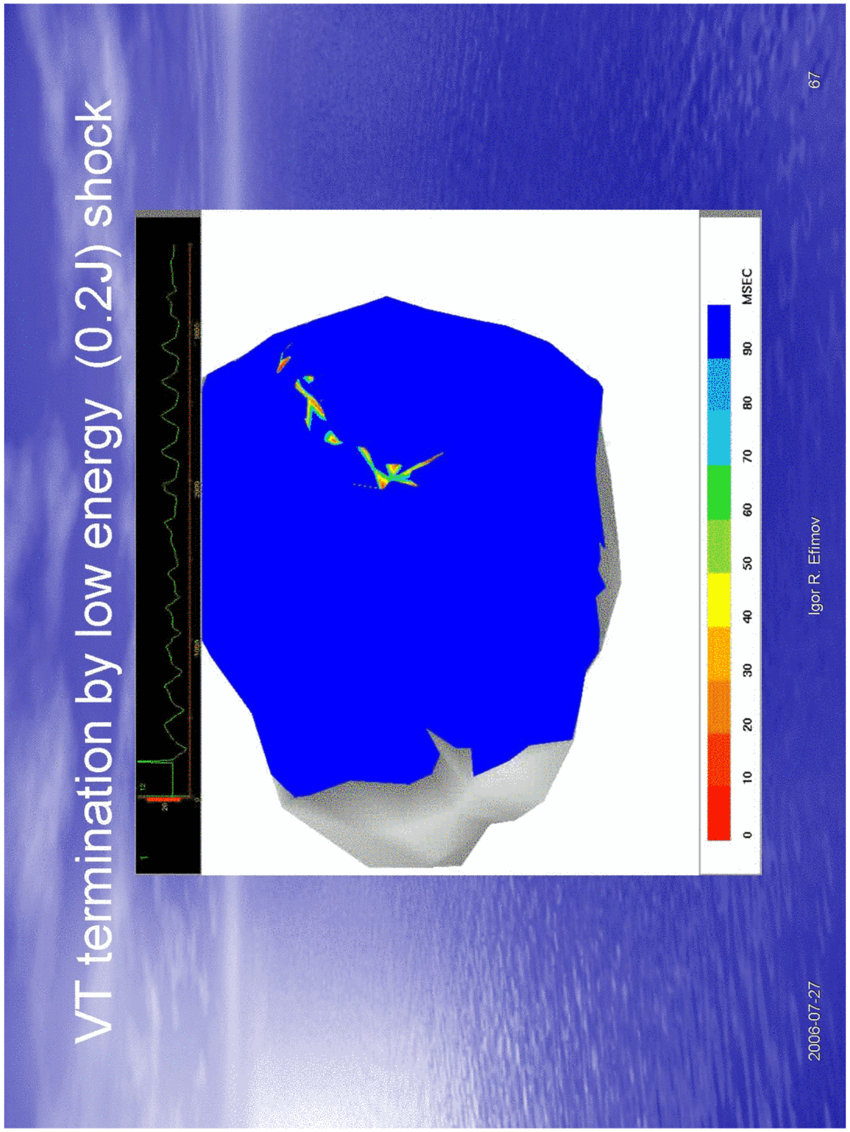
VT termination by low energy (0.2J) shock
MSEC
0 10 20 30 40 50 60 70 80 90
2006-07-27
Igor R. Efimov
67

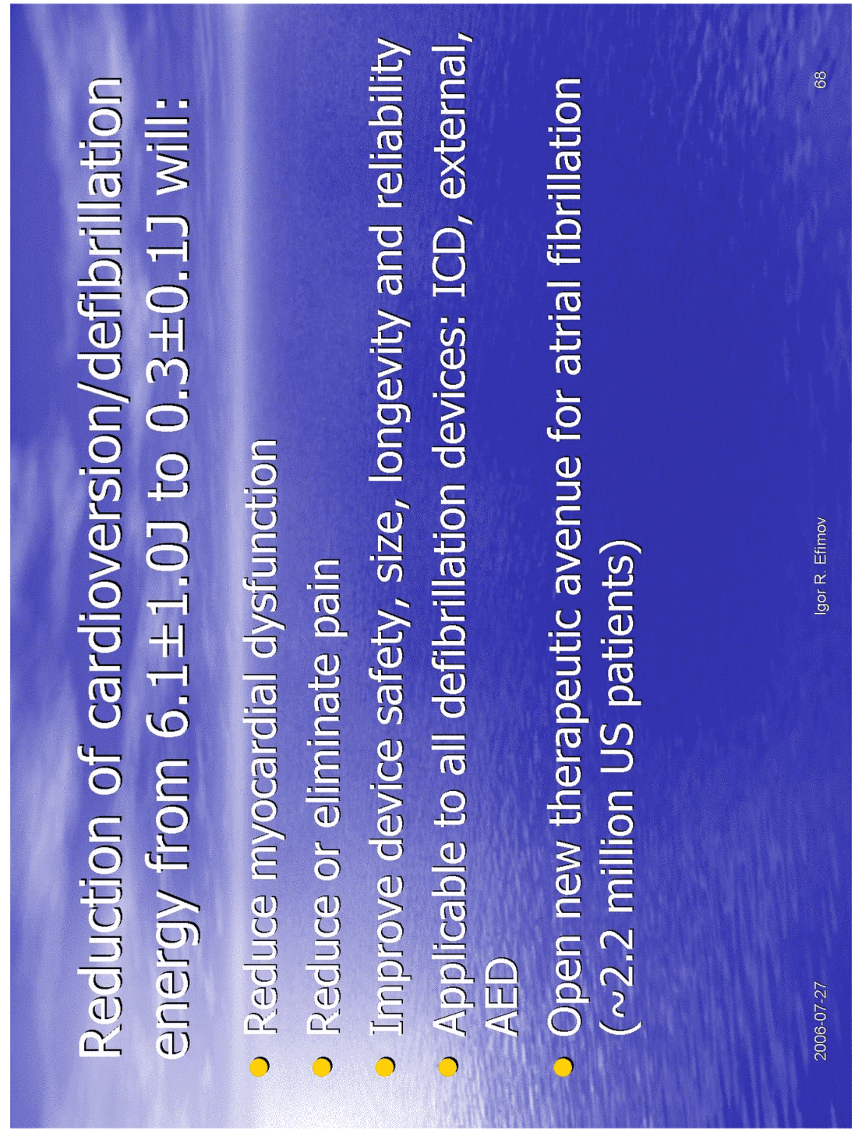
Reduction of cardioversion/defibrillation energy from 6.1±1.0J to 0.3±0.1J will:
Reduce myocardial dysfunction
Reduce or eliminate pain
Improve device safety, size, longevity and reliability
Applicable to all defibrillation devices: ICD, external, AED
Open new therapeutic avenue for atrial fibrillation (~2.2 million US patients)
2006-07-27
Igor R. Efimov
68


Acknowledgements
• Richard Schuessler lab (Washington University School of Medicine)
• Igor Efimov lab: Crystal Ripplinger, Vadim Fedorov, Fujian Qu (now SJM), Vladimir Nikolski (now MDT), Yuanna Cheng (now CCF), Alex Sambelashvili (now MDT), Li Li (now Ideker lab)
• Nice group: V.I. Krinski, A. Pumir, S. Takagi, D. Pazo
• National Institutes of Health, American Heart Association, Hartwell Foundation
2006-07-27
Igor R. Efimov
69